Sustainable urban logistics
A case study of waterway integration in Amsterdam

Pourmohammad-Zia, Nadia; van Koningsveld, Mark

DOI
10.1016/j.scs.2024.105334

Publication date
2024

Document Version
Final published version

Published in
Sustainable Cities and Society

Sustainable Cities and Society 105 (2024) 105334

Contents lists available at ScienceDirect

Sustainable Cities and Society

journal homepage: www.elsevier.com/locate/scs

Sustainable urban logistics: A case study of waterway integration in Amsterdam

Nadia Pourmohammad-Zia [a,*], Mark van Koningsveld [a,b]

[a] Department of Hydraulic Engineering, Delft University of Technology, The Netherlands
[b] Van Oord Dredging and Marine Contractors, 3068 NH Rotterdam, The Netherlands

ARTICLE INFO

Keywords:
Urban logistics
Modal shift
Waterways
Sustainability
Two-echelon location routing
Combinatorial optimization

ABSTRACT

This paper tackles the growing challenges in urban logistics by presenting an optimal distribution network that integrates urban waterways and last-mile delivery, tailored for cities boasting extensive waterway networks. We examine Amsterdam's city center as a case study, prompted by the strain on quay walls, congestion, and emissions, urging a reevaluation of its urban logistics design. We formulate the problem as a two-echelon location routing problem with time windows and introduce a hybrid solution approach for effective resolution. Our algorithm consistently outperforms existing methods, with a superior solution quality, demonstrating its effectiveness across established and newly developed benchmark instances. In our case study, we evaluate the benefits of transitioning from a roadway-centric to a waterway-based system, showcasing significant cost savings (approximately 28 %), reductions in vehicle weight (approximately 43 %), and minimized travel distances (approximately 80 %) within the city center. The integration of electric vehicles enhances environmental sustainability, resulting in a total daily emission reduction of 43.46 kg. Our study underscores the untapped potential of inland waterways in easing urban logistics challenges. Inspired by Amsterdam's experience, global cities can adopt innovative approaches for sustainable logistics, providing valuable insights for managers striving to enhance efficiency, cut costs, and promote sustainable transportation practices.

1. Introduction

Efficient urban logistics can be seen as a fundamental prerequisite for the economy and livability of the cities. The ever-increasing population in urban areas puts this efficiency under pressure and forces serious challenges such as congestion, emissions, noise, and safety issues on the other hand (Aloui et al., 2021). Accordingly, seeking innovative solutions to mitigate the adverse effects of urban logistics and improve its performance is imperative. One such solution lies in the exploration of alternative transportation modes. While road transport currently dominates urban freight, inland waterways present untapped potential in many cities worldwide, such as Amsterdam, Venice, Bangkok, Sydney, Utrecht, Stockholm, and Hamburg (Wojewódzka-Król & Rolbiecki, 2019).

In Amsterdam, the growing strain on public spaces, along with congestion and the considerable task of maintaining bridges and quay walls, has prompted the need to reassess the city's current logistics design (van der Does, 2019). The situation is particularly challenging in the historic center, where freight transport contributes to quay wall deterioration and congestion on the narrow roads alongside the canals (Korff et al., 2022). This balance between conserving heritage and accommodating new demands is a shared concern, not unique to Amsterdam. Many cities worldwide share the need for urgent action to safeguard their historical infrastructure while enhancing logistical networks. Historically, canals served as vital transportation routes in many city centers across the globe. However, over time, roadways gradually outcompeted waterways as the preferred mode of transportation. Thereby, the spatial correlation between the waterway and urban development was overlooked, leaving behind remnants of old quay walls and bridges.

Amsterdam's topological features make inland waterways integral to its logistical needs. The canals offer opportunities for a modal shift, particularly in construction material, waste, and food supplies (Nepveu & Nepveu, 2020). Construction material utilizes temporary barges as Transshipment Points (TPs) at project sites (van der Storm, 2021). Waste transfer to vessels is typically direct, while dedicated TPs are essential for food supplies (Municipality of Amsterdam MoA, 2020). Establishing these points involves factors beyond vessel routing and last-mile

* Corresponding author.
E-mail address: n.pourmohammadzia@tudelft.nl (N. Pourmohammad-Zia).

https://doi.org/10.1016/j.scs.2024.105334
Received 6 November 2023; Received in revised form 6 March 2024; Accepted 8 March 2024
Available online 12 March 2024

deliveries, encompassing space availability, extension viability, and infrastructure conditions like quay walls, bridges, and canal attributes. Infrastructural restrictions, spatial challenges, canal characteristics, and time-sensitive operations add layers of complexity to TP establishment.

Driven by the existing challenges, this study designs an optimal hotels, restaurants and café (HoReCa) logistics network for the historical center of Amsterdam. The network comprises a synergistic integration of urban waterways and last-mile delivery via road transportation. To this end, the problem is formulated as a two-echelon location routing problem with time windows (Contardo et al., 2012), where heterogeneous vessels in the first echelon and Moving Jacks together with light electric vehicles in the second echelon are applied. To tackle this intricate problem, a hybrid solution approach is devised, leveraging a custom-designed adaptive large neighborhood search (ALNS) (Ropke & Pisinger, 2006), local search techniques, K-means clustering (Kodinariya et al., 2013), and branch and price (Barnhart et al., 1998) methods. The proposed framework can efficiently mitigate the urban logistics challenges by eliminating heavy-duty vehicles from the city center and implementing electric vessels and light electric vehicles. This results in reduced congestion, and emissions, and alleviates strain on quay walls and bridges.

In addressing the underexplored domain of urban logistics within waterways, our study offers a distinctive contribution by designing an optimal logistics chain tailored explicitly for urban waterway distribution. This research stands out by considering specific canal classes, influencing distances between nodes for varying vessel sizes and shaping unique routing scenarios. Notably, we incorporate time limitations associated with vessel laying due to the physical constraints of waterborne navigation. Beyond conventional models, our paper introduces novel features often overlooked in urban distribution studies (see Table 1), including decisions on TP locations, integration of electric vehicles, synchronization considerations, and the use of Moving Jacks with light electric vehicles. To address the complexity of this multifaceted problem, our advanced solution algorithm combines the branch and price technique in the first tier with an adaptive large neighborhood search (ALNS) in the second tier. The ALNS, incorporating problem-specific destroy and repair operators, utilizes local search and K-means clustering techniques for robust solution intensification. This approach is adept at solving medium to large-sized instances of the problem, facilitating effective decision-making.

The structure of the subsequent sections is as follows: Section 2 reviews relevant literature, highlighting research gaps. Section 3 presents the problem description and mathematical model. The solution methodology is detailed in Section 4. Section 5 covers numerical results, the case study, sensitivity analysis, and discussion. Finally, Section 6 concludes the paper.

2. Literature review

In this section, we briefly review the existing literature on urban logistics, where operational planning and logistics chain design are particular points of interest. Our research mainly builds on two streams: the application of inland waterways in urban logistics and two-echelon routing in urban logistics, each of which will be reviewed as follows.

2.1. Application of inland waterways in urban logistics

Despite its potential, the literature on waterborne freight transport in urban logistics is fairly confined, and there are limited research works in this area. Janjevic and Ndiaye (2014), Maes et al. (2015), Miloslavskaya et al. (2019), and Wojewódzka-Król and Rolbiecki (2019) have reviewed successful practices of waterborne urban logistics worldwide. Several initiatives have been introduced in these papers such as Beer Boat in Utrecht, "Vracht door de gracht" (freight through canals) in Amsterdam, Vert Chez Vous in Paris, and Sainsbury's in London.

Kortmann et al. (2018) investigated the potential of waterborne

Table 1
General overview of the existing literature on 2E-VRP in urban logistics.

Reference	Location	satellite capacity	Time windows	Synchronization	Transport modes				Solution Approach
					Waterways	Moving jacks	Electric vehicles	UAVs	
Crainic et al. (2009)		✓	✓						HD
Grangier et al. (2016)			✓						ALNS
Belgin et al. (2018)		✓							VND+LS
Zhao et al. (2018)	✓	✓							CAH
Bevilaqua et al. (2019)									MA
Breunig et al. (2019)		✓					✓		LNS
Darvish et al. (2019)	✓	✓							B&P
Jie et al. (2019)		✓					✓		ALNS + *B&P*
Enthoven et al. (2020)									ALNS
Li et al. (2020)		✓	✓					✓	ALNS
Yu et al. (2020)			✓				✓		CH+LNS
Anderluh et al. (2021)				✓					LNS
Huang et al. (2021)		✓							GGH
Li et al. (2021)			✓	✓					ALNS
Mirhedayatian et al. (2021)	✓	✓	✓	✓					DBH
Vincent et al. (2021)			✓						ALNS
Wu and Zhang (2021)							✓		B&P
Jia et al. (2022)		✓	✓	✓					ALNS
Mhamedi et al. (2022)			✓						B&P
Akbay et al. (2022)			✓				✓		CH
Pina-Pardo et al. (2022)	✓	✓							SSA
Zhang et al. (2023)									HGA
Shi et al. (2023)	✓	✓							MO–HH
Liu et al. (2023)									C-AIA
This Study	✓	✓	✓	✓	✓	✓	✓		ALNS +LS+ *B&P*

* HD: Hierarchical Decomposition; ALNS : Adaptive Large Neighborhood Search; B&P: Branch and Price; VND: Variable Neighborhood Descent (VND); LS: Local Search; CAH: Cooperative Approximation Heuristic; MA: Memetic Algorithm; HGA: Hybrid Genetic Algorithm; LNS: Large Neighborhood Search; B&B: Branch and Bound; GGH: Graph-Guided Heuristic; DBH: Decomposition-Based Heuristic; CH: Construction Heuristic; SSA: sample average approximation; MO–HH: multi-objective hybrid heuristic; C-AIA: Cluster-based Artificial Immune Algorithm.

distribution for same-day delivery to shopkeepers in Amsterdam. They developed a simulation model to analyze the performance of this distribution system and determine the appropriate fleet size. Their results show that waterborne distribution with few hubs can be a competent and sustainable delivery mode in Amsterdam, provided that further studies on its financial viability are carried out.

Divieso et al. (2021) explored the viability of urban waterway logistics in Brazil, applying a comparative study to the city of Belém. Meanwhile, Nepveu and Nepveu (2020) investigated the potential of urban waterway transport in Amsterdam, examining key factors for success and failure in modal shifts. While these studies offer a foundational understanding, their insights serve as a guide for our research on the potential of waterways in urban logistics.

Gu and Wallace (2021) developed one of the few optimization models for waterborne urban logistics, a facet aligned with our paper. Focused on waterways, their mixed-integer programming model, exploring autonomous water-taxis in Bergen, Norway, addresses daily operational decisions. Diverging from their exclusive waterway concentration, our paper tackles a broader two-echelon network. While their results demonstrate the potential benefits of autonomous vessels, a solution approach is required to address real size problems. In next subsection, we will delve deeper into the common optimization models for urban logistics.

2.2. Two-Echelon routing problem in urban logistics

Two-Echelon Vehicle Routing Problem (2E-VRP) is an affluent area of academic research in urban logistics. Intermediate facilities, known as TPs or satellites are the points where the two echelons meet, applied for consolidation and transshipment of the items between the two tiers, and are an essential part of two-echelon networks. When these points are not pre-established, and their locations need to be determined, the problem turns into a two-echelon location routing problem (2E-LRP). Other variants of the problem, such as two-echelon inventory routing, truck-and-trailer routing, and production routing, are not the point of our interest in this paper.

Crainic et al. (2009) introduced the first 2E-VRP model in a multi-product and multi-depot setting. Zhou et al. (2018) extended this research into a multi-depot 2E-VRP with delivery options, allowing the customers to pick up their parcels at satellites. They developed a hybrid multi-population genetic algorithm to solve the problem. Belgin et al. (2018) studied a variant of the problem for which pick-up and deliveries are considered and applied this two-echelon distribution system in a supermarket chain in Turkey.

Li et al. (2020) investigated the application of unmanned aerial vehicles (UAVs) in the second echelon, where the first echelon vans are considered mobile satellites for UAVs. Enthoven et al. (2020) introduced covering locations in 2E-VRPs, from where customers can pick up their parcels. Similarly, Vincent et al. (2021) designed a two-echelon distribution system considering covering locations and occasional drivers. They showed that using crowds as occasional drivers in addition to the city freighters increases the efficiency of the distribution network.

Synchronizing the arrival and departure of the vehicles in the first and second echelons is essential in designing a seamless distribution network. Yet, this is mostly overlooked in the existing literature. Anderluh et al. (2021) provided one of the few works that took satellite synchronization into account. They considered synchronization in a multi-objective setting. In order to address the desires of citizens and municipalities, they applied a second objective function that accounts for the negative effects of transport, such as emissions. Li et al. (2021) and Jia et al. (2022) are the other researchers who took synchronization into account in their classic 2E-VRP.

The decision to establish TPs, leading to 2E-LRPs, increases the complexity of the already complex 2E-VRPs. Thereby, few papers have taken both locating and routing decisions into account. Among those are Zhao et al. (2018), Darvish et al. (2019), and Mirhedayatian et al. (2021), who have investigated 2E-LRP in capacitated, timely-flexible and synchronized settings, respectively. Two-echelon electric vehicle routing is the other extension of 2E-VRP, where the vehicles have a limited driving range. This assumption is heeded in three ways: limiting the traveled distance or considering refilling batteries at charging or battery swap stations. Breunig et al. (2019), Jie et al. (2019), and Wu and Zhang (2021) are examples of this extension.

Sluijk et al. (2023) provided a comprehensive review on recent advancements in the area of Two-echelon Vehicle Routing Problems. Interested readers are referred to this paper for further studies. Table (1) provides a general overview of the existing literature on the two-echelon routing problem in urban logistics, serving as a comparative reference for the features of each study.

Coming up with a general overview, the exploration of waterways as a viable option for urban logistics has received limited attention, highlighting a gap in the literature that our research significantly addresses. While previous studies have merely scratched the surface of waterway exploration in urban logistics, our paper distinguishes itself by presenting a detailed and tailored approach to designing an optimal logistics chain for urban waterway distribution. On the flip side, the two-echelon vehicle routing problem (2E-VRP) in urban logistics has attracted ample academic attention. However, numerous promising avenues have been undervalued or overlooked. Our paper fills these gaps by addressing crucial aspects such as optimal TP identification, synchronization for enhanced efficiency, integration of electric vehicles, consideration of multiple delivery modes, and harnessing the potential of waterways in the first echelon of transportation.

While holding promise as a sustainable logistics solution, waterways introduce additional intricacies to the issue. These encompass factors like infrastructural limitations (including waterway depth, width, bridge air draught, and maneuverability) and the space challenges posed by transshipment points and laying time. This modal shift further impacts the transport capacity, driving range, and delivery time, since vessels provide larger capacity, longer driving range and slower navigation. In our paper, we tackle these issues by fine-tuning the input parameters, deriving waterway distances based on canal classes, and integrating relevant constraints into the model. In this way, we uncover new insights and opportunities to promote a more sustainable and efficient urban logistics ecosystem.

3. Problem description and mathematical model

This paper considers a multi-modal two-echelon location and routing problem with time windows that rises in urban logistics. The network embraces a combination of inland waterways and streets. The first echelon involves the flow of inland vessels from a central hub to transshipment locations in the city center and then back to the hub. The transshipment locations are the points where the two echelons meet, the vessels are unloaded, and the last-mile delivery starts by Light Electric Vehicles (LEVs) with a maximum weight of 700 kg or Moving jacks with a maximum weight of 150 kg (Díaz-Ramírez et al., 2023). Each vessel can serve several TPs, and each TP can be visited by more than one vessel, implying that split delivery is admissible in the first echelon. The second echelon includes the flow of LEVs from vehicle depots to the transshipment locations and then navigating a prescribed route to serve designated demand points (HoReCa businesses) and finally returning to the depot. In mirroring real-world practices, Moving jacks are deployed to service demand points near transshipment locations, diverging from the use of LEVs.

The problem is modeled on a directed graph G(V, E), where V represents the set of vertices and E is the set of arcs. $V = V_1 \cup V_2$ includes the set of vertices in the first echelon (V_1) and second echelon (V_2). The set $V_1 = \{CH\} \cup TP$ involves the central hub (CH) and the transshipment locations (TP). The set $V_2 = VD \cup TP \cup HRC$ is comprised of the vehicle depots (VD), the transshipment locations (TP), and the demand points (HRC). $E = \{(i,j)| \ i,j \in V, \ i \neq j, \ (i,j) \in A \cup B\}$ where A

and B are the sets of admissible arcs for the first and second echelon, respectively. $A = A_1 \cup A_2$ and $B = B_1 \cup B_2 \cup B_3$ where:

$A_1 = \{(i,j) | \ i = CH, \ j \in TP\}$, $A_2 = \{(i,j) | \ i \in TP, \ j \in TP \cup \{CH\}\}$

$B_1 = \{(i,j) | \ i \in VD, \ j \in TP\}$, $B_2 = \{(i,j) | \ i \in TP, \ j \in HRC\}$, $B_3 = \{(i,j) | \ i \in HRC, j \in HRC \cup VD\}$

It should be noted that the distance between any two nodes in the first echelon, is not driven only based on the shortest path method but concerning different canal classes. Thereby, the distance between two identical nodes can differ for various vessel types with different sizes. Fig. (1) illustrates a typical solution on the described graph.

In order to complete the flow in the first echelon, we need to locate the transshipment points. These locations are specified from a set of potential sites for transshipment. The transshipment locations are assumed to be heterogeneous, implying that their establishment cost, capacity, and allowed laying time are different. Having the set of designated locations that are used by the vessels, LEVs, and Moving Jacks, the routing decisions of the vessels and LEVs are determined. The remainder of the notations which are used to formulate the model are as follows:

Parameters	
D_i	Demand of $i \in HRC$
S_i^{ID}	Service time of vertex i ($ID = I$ first echelon, $ID = II$ second echelon)
T_{ijk}^{ID}	Travel time of arc (i,j) for vehicle k ($ID = 1$ vessels, $ID = II$ LEVs)
T_{ij}^{III}	Travel time of arc (i,j) for Moving Jacks
AL_i	Allowed laying time at transshipment point i
TA_i	Lower bound for admissible service time at vertex i
TB_i	Upper bound for admissible service time at vertex i
CAP_i	Capacity of transshipment point $i \in TP$
Q_k^{ID}	Capacity of vehicle k ($ID = 1$ vessels, $ID = II$ LEVs)
DL_k^I	Driving range limit for vessel k
DL^{II}	Driving range limit for LEVs
C_{ijk}^{ID}	Cost of traveling arc (i,j) by vehicle k ($ID = 1$ vessels, $ID = II$ LEVs)
DIS_{ijk}^I	Average traveling distance of arc (i,j), $i,j \in V_1$ for vessel k
DIS_{ij}^{II}	Average traveling distance of arc (i,j), $i,j \in V_2$
DTr	Threshold distance to use Moving Jacks
FC_i	Period equivalent fixed cost of establishing transshipment point $i \in TP$
l_{ij}	1: if demand point $j \in HRC$ is located at a distance shorter than DTr from point $i \in TP$ 0: otherwise
$m_1, \ldots, m_6$	Lower bound for the left-hand side of the respective constraints
$M_1, \ldots, M_4$	Upper bound for the left-hand side of the respective constraints

(continued on next column)

(continued)

Decision variables	
x_{ijk}^I	1: if vessel $k \in K_1$ travels from $i \in V_1$ to $j \in V_1$ 0: otherwise
x_{ijk}^{II}	1: if LEV $k \in K_2$ travels from $i \in V_2$ to $j \in V_2$ 0: otherwise
u_{ij}	1: if the demand point $j \in HRC$ is served by a Moving Jack from transshipment point $i \in TP$ 0: otherwise
y_i	1: if transshipment point $i \in TP$ is established 0: otherwise
p_{ijk}	1: if the items of the demand point $j \in HRC$ are delivered by vessel $k \in K_1$ to $i \in TP$ 0: otherwise
$v_{k\hat{k}i}$	1: if LEV $\hat{k} \in K_2$ meets vessel $k \in K_1$ at $i \in TP$ 0: otherwise
st_{ik}^I	Time when vessel $k \in K_1$ starts to service vertex $i \in V_1$
st_{ik}^{II}	Time when LEV $k \in K_2$ starts to service vertex $i \in V_2$
st_{ij}^{III}	Time when a Moving Jack assigned to serve $j \in HRC$ starts to service vertex $i \in TP \cup HRC$
at_{ik}^I	Time when vessel $k \in K_1$ arrives at vertex i
q_{ik}	The amount delivered by vessel $k \in K_1$ to the transshipment point $i \in TP$
pu_{ijk}	Auxilary binary variable

Optimization Model

$$P_1 : min\ Z = \sum_{k\in K_1}\sum_{i\in V_1}\sum_{j\in V_1} C^I_{ijk} x^I_{ijk} + \sum_{k\in K_2}\sum_{i\in V_2}\sum_{j\in V_2} C^{II}_{ijk} x^{II}_{ijk} + \sum_{i\in TP} FC_i\, y_i \tag{1}$$

s.t.

$$\sum_{j\in TP} x^I_{ijk} \le 1 \qquad \forall i \in \{CH\},\ k \in K_1 \tag{2}$$

$$\sum_{i\in V_1} x^I_{ivk} - \sum_{j\in V_1} x^I_{vjk} = 0 \qquad \forall v \in TP,\ k \in K_1 \tag{3}$$

$$\sum_{i\in V_1} x^I_{ijk} \le y_j \qquad \forall j \in TP,\ k \in K_1 \tag{4}$$

$$at^I_{jk} = \sum_{i\in V_1}\left(st^I_{ik} + S^I_i + T^I_{ijk}\right) x^I_{ijk} \qquad \forall j \in V_1,\ k \in K_1 \tag{5}$$

$$st^I_{ik} \ge at^I_{ik} \qquad \forall i \in V_1,\ k \in K_1 \tag{6}$$

$$st^I_{ik} + S^I_i - at^I_{ik} \le AL_i \qquad \forall i \in TP,\ k \in K_1 \tag{7}$$

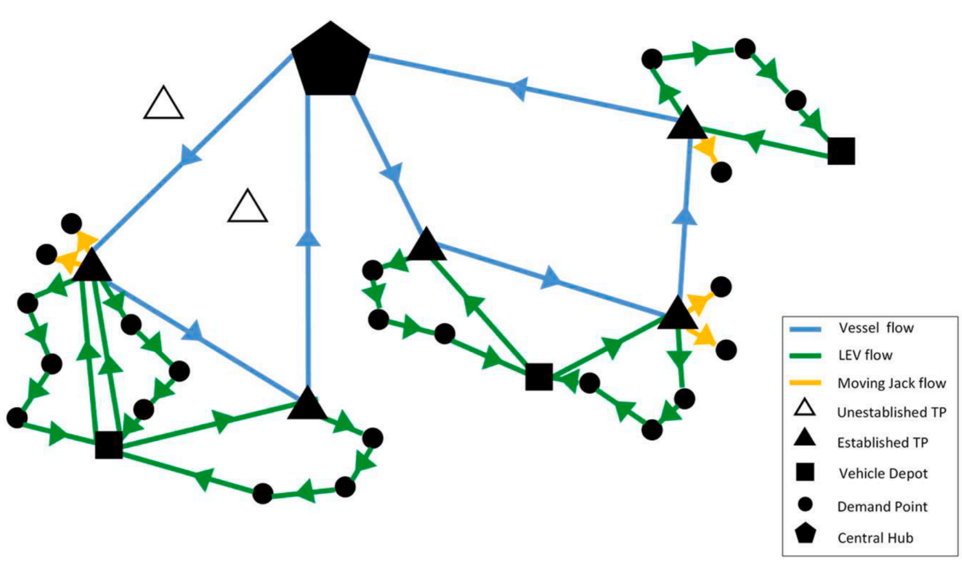

Fig. 1. The graph of the problem.

$$\sum_{i\in TP} q_{ik} \le Q_k^I \qquad \forall k \in K_1 \tag{8}$$

$$q_{jk} \le M_1 \sum_{i\in V_1} x_{ijk}^I \qquad \forall j \in TP,\ k \in K_1 \tag{9}$$

$$q_{ik} = \sum_{j\in HRC} D_j\ p_{ijk} \qquad \forall i \in TP,\ k \in K_1 \tag{10}$$

$$\sum_{k\in K_1}\sum_{i\in TP} p_{ijk} = 1 \qquad \forall j \in HRC \tag{11}$$

$$p_{ijk} \le \sum_{v\in V_1} x_{vik}^I \qquad \forall i \in TP,\ k \in K_1 \tag{12}$$

$$\sum_{k\in K_1}\sum_{j\in HRC} D_j\ \ p_{ijk} \le CAP_i \qquad \forall i \in TP \tag{13}$$

$$DTr - DIS_{ij} \le M_2 l_{ij} \qquad \forall i \in TP, j \in HRC \tag{14}$$

$$DTr - DIS_{ij} \ge m_1\left(1 - l_{ij}\right) \qquad \forall i \in TP, j \in HRC \tag{15}$$

$$\sum_{k\in K_1} p_{ijk} + l_{ij} \le 1 + u_{ij} \qquad \forall i \in TP, j \in HRC \tag{16}$$

$$\sum_{k\in K_1} p_{ijk} + l_{ij} \ge 2u_{ij} \qquad \forall i \in TP, j \in HRC \tag{17}$$

$$\sum_{i\in VD}\sum_{j\in V_2} x_{ijk}^{II} \le 1 k \in K_2 \tag{18}$$

$$\sum_{i\in V_2} x_{ijk}^{II} \le y_j \qquad \forall j \in TP,\ k \in K_2 \tag{19}$$

$$\sum_{i\in V_2} x_{ivk}^{II} - \sum_{i\in V_2} x_{vjk}^{II} = 0 \qquad \forall v \in TP \cup HRC,\ k \in K_2 \tag{20}$$

$$\sum_{k\in K_2}\sum_{i\in V_2} x_{ijk}^{II} + \sum_{i\in V_2} u_{ij} = 1 \qquad \forall j \in HRC \tag{21}$$

$$\sum_{i\in V_2}\sum_{j\in V_2} DIS_{ijk}^I\ x_{ijk}^I \le DL_k^I \qquad \forall k \in K_1 \tag{22}$$

$$\sum_{i\in V_2}\sum_{j\in V_2} DIS_{ij}^{II}\ x_{ijk}^{II} \le DL^{II} \qquad \forall k \in K_2 \tag{23}$$

$$\sum_{i\in V_2}\sum_{j\in V_2} D_j\ \ x_{ijk}^{II} \le Q_k^{II} \qquad \forall k \in K_2 \tag{24}$$

$$st_{ik}^{II} \ge \left(st_{ik}^{II} + S_i^{II} + T_{ijk}^{II}\right)x_{ijk}^{II} \qquad \forall i,j \in V_2,\ k \in K_2 \tag{25}$$

$$st_{jj}^{III} = \left(st_{ij}^{III} + S_i^{II} + T_{ij}^{III}\right)u_{ij} \qquad \forall i \in TP, j \in HRC \tag{26}$$

$$st_{i\hat{k}}^{II} - st_{ik}^{I} - S_i^{I} \ge m_2\left(1 - v_{k\hat{k}i}\right) \qquad \forall i \in TP,\ k \in K_1, \hat{k} \in K_2 \tag{27}$$

$$st_{ij}^{III} - st_{ik}^{I} - S_i^{I} \ge m_3\left(1 - pu_{ijk}\right) \qquad \forall i \in TP, j \in HRC,\ k \in K_1 \tag{28}$$

$$p_{ijk} + u_{ij} \le 1 + pu_{ijk} \qquad \forall i \in TP, j \in HRC,\ k \in K_1 \tag{29}$$

$$p_{ijk} + u_{ij} \ge 2pu_{ijk} \qquad \forall i \in TP, j \in HRC,\ k \in K_1 \tag{30}$$

$$v_{k\hat{k}j} \le \sum_{i\in V_1} x_{ijk}^I \qquad \forall j \in TP,\ k \in K_1, \hat{k} \in K_2 \tag{31}$$

$$\sum_{k\in K_1} v_{k\hat{k}i} = \sum_{j\in V_2} x_{ij\hat{k}}^{II} \qquad \forall i \in TP,\ \hat{k} \in K_2 \tag{32}$$

$$\sum_{k\in K_1}\sum_{i\in TP} v_{k\hat{k}i} \le 1 \qquad \forall \hat{k} \in K_2 \tag{33}$$

$$\sum_{\hat{k}\in K_2} v_{k\hat{k}i} + pu_{ijk} \ge p_{ijk} \forall i \in TP, j \in HRC,\ k \in K_1 \tag{34}$$

$$TA_j \sum_{i\in V_2} x_{ijk}^{II} \le st_{jk}^{II} \le TB_j \sum_{i\in V_2} x_{ijk}^{II} \qquad \forall j \in HRC,\ k \in K_2 \tag{35}$$

$$TA_j \sum_{i\in TP} u_{ij} \le st_{jj}^{III} \le TB_j \sum_{i\in TP} u_{ij} \qquad \forall j \in HRC \tag{36}$$

$$x_{ijk}^I, x_{ijk}^{II},\ y_i,\ p_{ijk},\ v_{k\hat{k}i}, u_{ij},\ pu_{ijk}\ \in \{0,1\} \forall i,j \in V,\ k \in K \tag{37}$$

$$st_{ik}^I, st_{ik}^{II}, st_i^{III},\ q_{ik} \ge 0 \forall i,j \in V,\ k \in K \tag{38}$$

(1): The objective function - to minimize total costs involving travel and period equivalent establishment cost.
(2): Each vessel departs from the central hub at most once.
(3): First echelon flow constraints.
(4): A TP can only be visited if it is established.
(5)-(6): Consistency of arrival and service times.
(7): Admissible laying times.
(8): Vessel capacity limits.
(9): The delivery volume of vessel to a TP could be non-zero, only if that vessel visits the mentioned TP.
(10): Quantities delivered to a TP should satisfy the demand.
(11): Each demand point is served by one TP.
(12): A TP can serve a demand point only if it is established.
(13): Capacity limits of TPs.
(14)-(17): The allocation of Moving Jacks to demand points in proximity to TPs.
(18): Each can LEV depart from one of the vehicle depots and at most once.
(19): An LEV can access a TP only if it that TP has been established.
(20): Flow constraints in the second echelon.
(21): Each demand point is served either by an LEV or a Moving Jack.
(22): Limited driving range of vessels.
(23): Limited driving range of LEVs.
(24): Capacity limits of LEVs.
(25)-(26): Consistency in the service times of LEVs and Moving Jacks.
(27)-(28): Synchronization constraints, ensuring consistency in service times when vessels are synchronized with LEVs or Moving Jacks.
(29)-(30): Synchronization process between vessels and Moving Jack.
(31)-(34): Synchronization process between vessels and LEVs.
(35)-(36): Time windows.
(37)-(38): Types of variables used.

For readers with limited expertise in mathematical programming, please refer to Appendix A for a comprehensive explanation of the equations.

Eqs. (5), (25), and (26) are non-linear and are linearized as follows:

$$at_{jk}^I - st_{ik}^I - S_i - T_{ijk}^I \ge m_4\left(1 - x_{ijk}^I\right) \qquad \forall i,j \in V_1,\ k \in K_1 \tag{39}$$

$$at_{jk}^I - st_{ik}^I - S_i - T_{ijk}^I \le M_3\left(1 - x_{ijk}^I\right) \qquad \forall i,j \in V_1,\ k \in K_1 \tag{40}$$

$$st_{jk}^{II} - st_{ik}^{II} - S_i - T_{ijk}^{II} \ge m_5\left(1 - x_{ijk}^{II}\right) \qquad \forall i,j \in V_2,\ k \in K_2 \tag{41}$$

$$st_{jj}^{III} - st_{ij}^{III} + S_i - T_{ij}^{III} \ge m_6\left(1 - u_{ij}\right) \qquad \forall i \in TP, j \in HRC \tag{42}$$

$$st_{jj}^{III} - st_{ij}^{III} - S_i - T_{ij}^{III} \le M_4\left(1 - u_{ij}\right) \qquad \forall i \in TP, j \in HRC \tag{43}$$

Where constraints (39) and (40) are linearized versions of constraint (5) and constraints (41) are of constraint (25). Constraints (26) are linearized by constraints (42) and (43).

4. Solution methodology

Our Two-Echelon Location Routing problem is solved by a hybrid solution algorithm that decomposes the problem into two nested subproblems, including the first echelon and second echelon problems. We first develop an Adaptive Large Neighborhood Search (ALNS) metaheuristic to determine the location and routing decisions in the second echelon (Interested readers are referred to Ropke and Pisinger (2006) for a comprehensive understanding). Then, based on the provided results, we apply a Branch and Price (B&P) algorithm using the Dantzig-Wolfe decomposition principle to transform the first echelon routing model into a master problem and a subproblem (Interested readers are referred to Barnhart et al. (1998) for a comprehensive understanding of this method). Algorithm 1. provides the pseudocode of our proposed solution methodology and Fig. (2) illustrates its flowchart.

By applying the initial solution (S_{in}), our developed ALNS optimizes the decisions to be made for the second echelon (S_f^2). Then, based on the provided solution, the time windows and aggregated demand for the established points are derived. The procedure re-iterates until the termination criteria are met. The termination criteria are to reach the maximum number of iterations ($\mathbb{T}_G$) or the maximum number of iterations with no improvement. To enhance the performance of our solution approach, we first apply preprocessing, where we remove non-admissible arcs in the second echelon concerning time windows and vehicle capacity constraints.

4.1. Feasibility and penalty calculation

Our developed ALNS allows infeasible solutions to be a part of the search procedure and applies penalties for vehicle capacity, transshipment location capacity, and time windows violations. The generalized cost function of a solution S is formulated as:

$$f_{gen}\ (S) = \text{ obj} + \varrho_1 V^v_{Cap}(S) + \varrho_2 V^t_{Cap}(S) + \varrho_3 V_{TW}(S) + \varrho_4 V_{Dis}(S) \tag{44}$$

Where obj is the objective function (Eq. (44)) and the violations of vehicle capacity ($V^v_{Cap}(S)$), transshipment point capacity ($V^t_{Cap}(S)$), time windows ($V_{TW}(S)$), and driving range are scaled by the penalty weights $\varrho_1, \varrho_2, \varrho_3$ and ϱ_4, respectively. At intervals of every ψ_P iterations, denoted as the penalty update period, dynamic adjustments are made to the penalty weights. If a constraint is violated in a minimum of $\mathscr{L}^{\psi_P}$ out of ψ_P iterations, its associated penalty weight undergoes multiplication by ω_i. Conversely, if the constraint is satisfied in at least $\mathscr{L}^{\psi_P}$ iterations, the penalty weight is divided by the same value. To regulate the magnitude of f_{gen}, constraints on penalty factors are imposed to ensure they remain within specified minimum and maximum values. As stated by Schneider et al. (2013) the penalty weights experience an initial increase during the early iterations of the algorithm and progressively decrease as the solution converges.

Efficient calculation of the changes in cost function plays a crucial role in the performance of our algorithm. The changes in capacity and driving range violations are trivially obtained in $\mathscr{O}(1)$. In order to calculate the time windows violations, we incorporate the approach proposed by Nagata et al. (2010). Based on this approach, the violations in a node do not propagate to subsequent nodes of a sequence. As service time at different vertices is independent of the route sequence, the changes in time windows violations can be calculated in $\mathscr{O}(1)$.

4.2. Initial solution

A route in the second echelon starts from a vehicle depot, heads to a transshipment location, then navigates through several demand points, and finally returns to the initial vehicle depot. A solution for the second echelon is comprised of several routes, and each route is represented by a series of points $\langle VD_n, TP_m, HRC_1, \ldots, HRC_i, \ldots, HRC_k, VD_n \rangle$, where VD_n is the starting and ending depot for the route, TP_m is the selected and established transshipment point, and $HRC_1, \ldots, HRC_i, \ldots, HRC_k$ are the covered demand points within this route.

Barreto et al. (2007), Wang et al. (2018), and Akpunar and Akpinar (2021) have demonstrated the efficacy of clustering approaches in yielding high-quality solutions for capacitated location routing problems. Various clustering algorithms, such as DBSCAN, Gaussian Mixture, and K-means, exist in the literature. Despite its straightforward approach, K-means has exhibited notable performance in clustering spatial data, as evidenced by Akpunar and Akpinar (2021). Consequently, we employ the K-means clustering algorithm to determine the number and locations of transshipment points in our initial solution.

In our algorithm, selecting the number of clusters is a pivotal step, as our analysis indicates its impact on the quality of initial solutions. After meticulous examination, we initially set K as the estimated lower bound on required transshipment points, derived by dividing the total demand by the average transshipment location capacity. Cluster centers are chosen and updated from the set of potential candidates for locating transshipment points. Once demand points are assigned to these clusters, the required items' volume at each TP (cluster center) is obtained. If the capacity of at least one TP is violated by over 25 % (which is selected after careful sensitivity analysis), the number of clusters is increased by one, and K-means is re-iterated. Once the established transshipment points are finalized, the closest depot to each point is selected as the starting and ending depot of the vehicles serving that transshipment point.

By having the established transshipment points, the demand points located within a distance of Tr, which will be served by Moving Jacks, are specified and removed from the set of uncovered demand points. In order to complete the remainder of each route, we apply the semi-parallel construction (SPC) heuristic. As proposed by Paraskevopoulos et al. (2008), the parallel mechanism inherent in SPC generates non-myopic and high-quality initial solutions. This characteristic is the primary reason for our selection of this approach.

SPC is an iterative approach. At each iteration, we create the most promising candidate route for every currently available established TP (cluster). The selection of the best cluster-route is then made, and this process repeats until all demand points are covered. When considering insertion candidates for each cluster, the set of uncovered demand points is narrowed down from the global set to those within that cluster and its neighboring clusters. For a given cluster i, its neighboring clusters are defined as those clusters with at least one initially assigned demand point (identified by K-means) located within a maximum distance from the centroid of cluster i. The neighboring clusters are introduced because our initial choice of formed clusters can influence the routes constructed, making it essential to consider points not only within the cluster itself but also in its immediate surroundings.

An LEV for each cluster is taken to serve uncovered demand points. For each LEV, a route covering a part of uncovered demand points is constructed based on a greedy approach, taking capacity constraints into account. For diversification, we take a restricted candidate list (RCL)[1] of n demand points with the highest evaluation score and apply Roulette wheel selection[2] to select and insert a point. After constructing the routes, the best cluster-route is selected, and its covered customers are removed from the set of global uncovered points. The procedure iterates until no further uncovered points are left. The best cluster-route in each iteration has the lowest Average Cost per Unit Transferred, dividing

[1] A mechanism that limits the set of candidate elements considered for inclusion in a solution during the search process.

[2] A probabilistic technique used to choose a candidate solution from a set of solutions based on their fitness scores

Algorithm 1. The Two-Echelon Location Routing Algorithm

Input: Input Parameters Data	
Output: Best-found feasible solution (S_f^*)	
$Obj(S_f^*) = \infty$	*The best feasible solution is set to infinity*
Generate the initial solution for the 2nd echelon $S_{in}^2 \leftarrow SPC(input\ parameters)$	*The initial solution for the last-mile delivery is generated by SPC (S_{in}^2)*
Based on S_{in}^2 generate the initial solution for the 1st echelon $S_{in}^1 \leftarrow B\&P(S_{in}^2)$	*Having S_{in}^2 as the input, the initial solution of the waterway tier is generated (S_{in}^1)*
$S_{in} = \{S_{in}^1, S_{in}^2\}$	
while termination criteria are not met	*The loop iterates until the maximum iterations or the maximum iterations with no improvement is reached*
$S_f^{2*} \leftarrow ALNS(S_{in}^2)$ Apply ALNS to generate the best feasible solution for the 2nd echelon	*The best feasible solution of the 2nd echelon is obtained by ALNS (S_f^{2*})*
$S_f^{1*} \leftarrow B\&P(S_f^{2*})$ Based on S_f^{2*} generate the best feasible solution for the 1st echelon applying B&P	*Having S_f^{2*} as the input, the best feasible solution of the 1st echelon is obtained by B&P (S_f^{2*})*
$S_f = \{S_f^{1*}, S_f^{2*}\}$	*S_f^{1*}, S_f^{2*} form the feasible solution of the entire chain (S_f)*
if $Obj(S_f) \leq Obj(S_f^*)$	*If S_f provides a better solution the best feasible solution is updated.*
$S_f^* \leftarrow S_f$	
end if	
$S_{in} \leftarrow S_f$	*S_f is set as the initial solution and the loop reiterates*
end while	
return S_f^*	

associated costs by demand summation of visited points.

4.3. Adaptive large neighborhood search

We have taken ALNS as the core of our solution algorithm for the second echelon and adapted it to fit into our problem by allowing infeasible solutions, incorporating problem-specific destroy and repair operators, and applying local search for intensification. In order to enhance the speed of our algorithm, the potential demand points for insertion in repair and local search operators are selected from the original cluster or its neighboring clusters (see Section 4.2). That is, a demand point that is considerably far from a transshipment location cannot be served by that TP. The overview of our proposed ALNS is illustrated through Algorithm 2.

The termination criteria are to reach the maximum number of iterations ($\mathbb{T}_m$) or maximum number of iterations with no improvement ($\mathbb{T}_{n-m}$).

Destroy** and **Repair Operators

We have two types of destroy operators. The first, with a large impact, changes a part of the problem's configuration by removing transshipment points, and the second, with a small impact, affects only a part of the constructed routes. A destroy operator removes at least $\mathscr{G}$ nodes from the current solution, where $\mathscr{G}$ is a percentage of all nodes. This percentage is randomly drawn from a given interval $[\Lambda_{min}, \Lambda_{max}]$. In addition to the well-known Random, Worst, and Shaw and Route removal, we use the following destroy operators with a large impact.

- *Transshipment point removal* is introduced by Hemmelmayer et al. (2012), where a transshipment point is chosen randomly from the list of open ones and gets closed. Therefore, all routes originating from this TP are removed, adding their covered demand points together with points served by Moving Jacks from that TP to the customer pool. Furthermore, a TP is randomly chosen, and if it is not already established is opened. This prevents situations in which all transshipment points would be closed.
- *Transshipment point opening* is introduced by Hemmelmayer et al. (2012), where we choose a transshipment point randomly among unestablished ones and open it.
- *Transshipment point swap* is introduced by Hemmelmayer et al. (2012), where the TP removal operator is applied first. Then, we use a restricted candidate list (RCL) of n unestablished clusters with the shortest distance from the removed TP and apply a roulette wheel selection to select and establish a new transshipment location.

Our ALNS applies Greedy insertion, Regret insertion and SPC-based insertion, which modifies the SPC heuristic of the construction phase by inserting demand points to existing and new routes, provided that capacity constraints are met.

Local Search

To further improve the results of the destroy and repair operators, a Local Search (LS) is applied that uses a composite neighborhood, including the well-known 2-opt (Potvin & Rousseau, 1995), 2*-opt (Potvin & Rousseau, 1995), Reinsertion (Savelsbergh, 1992), and Swap($n-1$), where $n = 1, \ldots, 4$ (Savelsbergh, 1992) moves.

Acceptance Criteria

We apply Simulated Annealing (SA)-based acceptance criteria in our developed ALNS: If a solution is improving, always accept it. Decide about non-improving (deteriorating) solutions based on a probability that depends on the amount of solution deterioration and the temperature following a cooling scheme.

Adaptive Mechanism

The destroy and repair operators are selected using a roulette wheel mechanism. The selection probability of each operator relies on its historical performance, which is projected by a weight. These weights are equal at the beginning of the algorithm and are updated after each ψ_L iterations. The weight of an operator i in adaption period t is updated as:

$$\mathscr{W}_{it} = \theta \frac{\mathrm{SN}_{it}}{\mathrm{NN}_{it}} + (1-\theta)\,\mathscr{W}_{i\ t-1} \tag{45}$$

Where θ is the smoothing factor, SN_i shows the success score of the

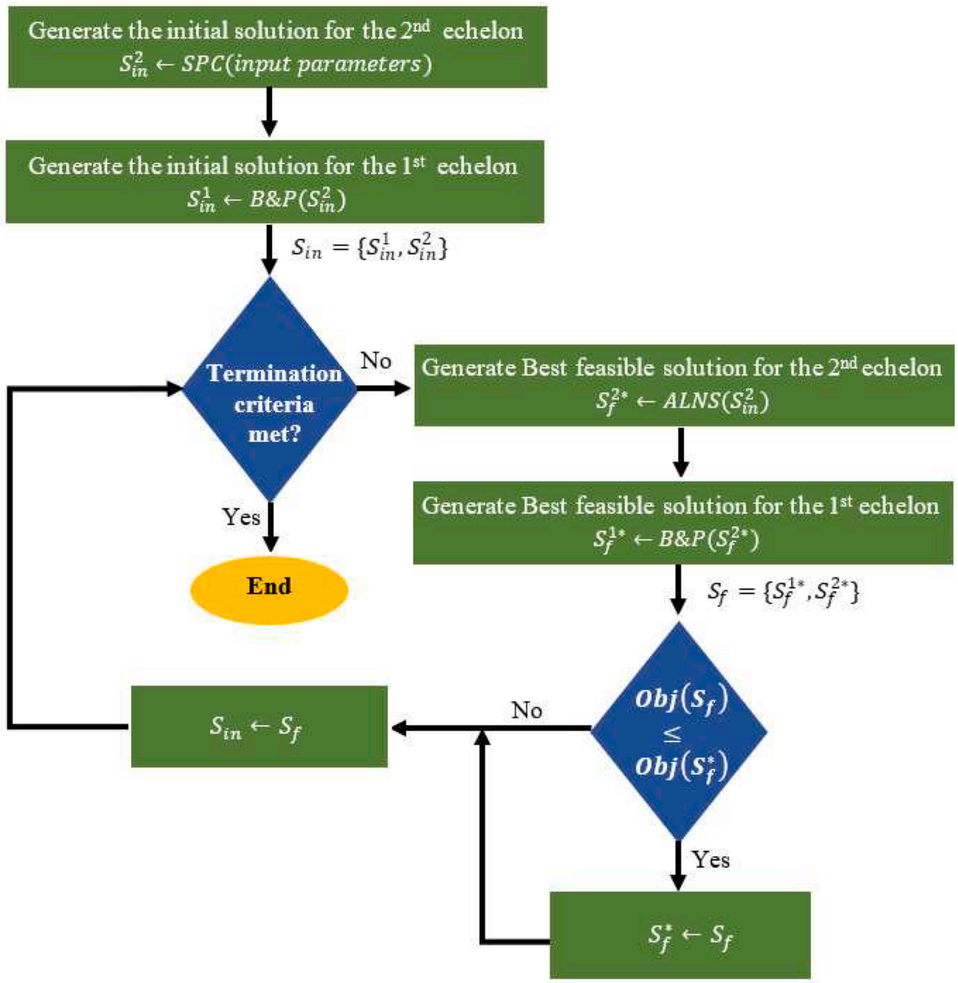

Fig. 2. Flowchart of the solution algorithm.

operator in the current update period and NN_{it} reflects the number of times the operator has been applied in update period t. In each update period, SN_{it} is initially set to zero and is updated by a scoring scheme using

$$SN_{it} = SN_{it} + \sigma_i, \ i = 1, 2, 3.$$

4.4. Branch and price

Once the solution of the second echelon is obtained, the problem at the first echelon is seen as a split delivery vehicle routing problem with time windows, where all waterway-specific constraints initially present in the mathematical model persist. The established transshipment points are treated as the demand points, requiring us to specify the demand and the time windows at these TPs. Since split deliveries are admissible, we cannot treat the set of all allocated demand points of a TP as a unit point. This is because all points visited by a single LEV should be served by a unique vessel due to synchronization constraints. Accordingly, we will have the accumulation of demands served by each LEV as one unique demand, located at its initial TP and with time windows respecting the time windows of all those demand points. Then, we need to create copies of TPs with demands equal to the demand of points served by a Moving Jack or accumulated demand of each LEV. This potentially can lead to many serving points with the same location and thereby high degeneracy of the problem. In order to mitigate this, demand points can be merged under certain conditions. Since split delivery was to resolve the problem of limited vessel capacity and considerably different time windows, the following model can be applied to merge the points in an efficient way for each TP:

Parameters	
CAP	A percentage of the smallest vessel's capacity (e.g., 25 %)
TR	The threshold for the difference in time windows
Decision variables	
μ_i	1: if group $i \in I$ is formed 0: otherwise
λ_{ij}	1: if point $j \in J$ is merged into group $i \in I$ 0: otherwise

$$P_2 : \boldsymbol{min}\ \boldsymbol{Z} = \sum_{i \in I} \mu_i \tag{46}$$

s.t.

$$\sum_{j \in J} D_j \lambda_{ij} \leq CAP.\mu_i \qquad \forall i \in I \tag{47}$$

$$\sum_{i \in I} \lambda_{ij} = 1 \qquad \forall j \in J \tag{48}$$

$$|TA_j - TA_{j'}| \lambda_{ij} \lambda_{ij'} \leq TR \qquad \forall i \in I, \ j, j' \in J \tag{49}$$

$$|TB_j - TB_{j'}| \lambda_{ij} \lambda_{ij'} \leq TR \qquad \forall i \in I, \ j, j' \in J \tag{50}$$

$$\mu_i, \ \lambda_{ij} \in \{0, 1\} \qquad \forall i \in I, \ j \in J \tag{51}$$

Algorithm 2. ALNS

Pseudocode	Explanation
Input: Initial Solution (S_{in}^2) obtained by SPC	*Take the initial solution obtained by SPC as the input*
Output: Best feasible solution for the second echelon (S_f^{2*})	
$S^2 \leftarrow S_{in}^2$ and $S^{2*} \leftarrow S_{in}^2$	*The initial solution is set as the best solution (S^{2*}) and current accepted solution (S^2)*
if S_{in}^2 is feasible	*If this solution is feasible, it is set as the best feasible solution (S_f^{2*})*
$\quad S_f^{2*} \leftarrow S_{in}^2$	
end if	
$i, j \leftarrow 0$	
while termination criteria are not met	*The loop reiterates until the maximum iterations or the maximum iterations with no improvement is reached*
$\quad S^{2'} \leftarrow$ Destroy&Repair (S^2)	*Destroy and repair operators are applied to get the current solution ($S^{2'}$)*
$\quad S^{2'} \leftarrow$ LocalSearch ($S^{2'}$)	*Local search is applied to intensify the current solution*
$\quad$ **if** $S^{2'}$ is accepted	*If $S^{2'}$ is accepted the accepted current solution is updated*
$\quad\quad S^2 \leftarrow S^{2'}$	
$\quad\quad$ **if** $f_{gen}(S^{2'}) \le f_{gen}(S^{2*})$	*In that case, if $S^{2'}$ improves the objective function, the best solution is updated*
$\quad\quad\quad S^{2*} \leftarrow S^{2'}$	
$\quad\quad$ **end if**	
$\quad\quad$ **if** $S^{2'}$ is feasible **and** $f_{gen}(S^{2'}) \le f_{gen}(S_f^{2*})$	*In that case, if $S^{2'}$ is feasible and improves the objective function of the best feasible solution, the best feasible solution is updated.*
$\quad\quad\quad S_f^{2*} \leftarrow S^{2'}$	
$\quad\quad\quad j \leftarrow i$	
$\quad\quad$ **end if**	
$\quad$ **end if**	
$\quad$ UpdateScore($S^{2'}$)	*Update the success scores of destroy and repair operators*
$\quad$ **if** $0 \equiv (i+1) \ mod(\psi_P)$	*If ψ_P iterations is passed from the last penalty update, update the penalty weights.*
$\quad\quad$ UpdatePenalty($S^{2'}$)	
$\quad$ **end if**	
$\quad$ **if** $0 \equiv (i-j+1) \ mod(\psi_R)$	*If ψ_R iterations is passed from the last replacement, replace the current accepted solution by the best solution.*
$\quad\quad S^2 \leftarrow S^{2*}$	
$\quad$ **end if**	
$\quad$ **if** $0 \equiv (i+1) \ mod(\psi_L)$	*If ψ_L iterations is passed from the last selection score update, update the selection scores of destroy and repair operators.*
$\quad\quad$ AdaptSelectionScores()	
$\quad$ **end if**	
$\quad i \leftarrow i+1$	
end while	
return S_f^{2*}	

The[3] problem is a variant of the bin packing problem for which a strong valid inequality exists as follows (Correia et al., 2008).

$$\lambda_{ij} \le \mu_i \qquad \forall i \in I,\ j \in J \tag{52}$$

$$\sum_{i\in I} \mu_i \ge |I| - r + 1 \qquad \forall i \in I,\ j, j' \in J \tag{53}$$

Where $|I|$ is the size of potential groups, and r is a value satisfying the following inequality:

$$(|I| - r - 1)CAP < \sum_{j\in J} D_j \le (|I| - r)CAP \qquad \forall i \in I,\ j, j' \in J \tag{54}$$

[3] Constraints (49) and (50) are non-linear and can be linearized as:

$(TA_j - TA_{j'})\eta_{ijj'} \le TR$	$\forall i \in I,\ j, j' \in J$
$(TA_{j'} - TA_j)\eta_{ijj'} \le TR$	$\forall i \in I,\ j, j' \in J$
$(TB_j - TB_{j'})\eta_{ijj'} \le TR$	$\forall i \in I,\ j, j' \in J$
$(TB_{j'} - TB_j)\eta_{ijj'} \le TR$	$\forall i \in I,\ j, j' \in J$
$\lambda_{ij} + \lambda_{ij'} \le 1 + \eta_{ijj'}$	$\forall i \in I,\ j, j' \in J$
$\lambda_{ij} + \lambda_{ij'} \ge 2\ \eta_{ijj'}$	$\forall i \in I,\ j, j' \in J$

Since the capacity of TPs is limited, the size of J for each TP is rather confined. Therefore, applying this valid inequality, the problem can be solved to optimality in a reasonable time.

In this way, the problem at the first echelon is transformed into a classic VRP with time windows, to solve which there exists extensive research applying branch and price. It works based on Dantzig Wolfe Decomposition, where the main optimization problem is decomposed into a master and several sub-problems (see Desaulniers et al. (2006) for details). It exploits the fact that in a classic VRP with time windows, the constraint associated with serving the demand point with one of the existing vehicles is the only constraint linking the vehicles together. By neglecting this constraint, the problem can be decomposed into sub-problems (each for one vehicle) that take the form of the shortest path problem with resource constraint (time windows and vehicle capacities).

5. Numerical results

In this section, we provide the results of the conducted numerical experiments. As illustrated in Table (1), the problem is new, for which no benchmark instances exist. Accordingly, the experiments are carried out on our newly-generated benchmark instances. Furthermore, we assess the performance of our developed solution approach on the available benchmark instances for 2E-VRP. Finally, a case study is presented to illustrate the results of the problem in a practical setting for the city of Amsterdam, followed by sensitivity analysis on the input parameters and discussion.

The experiments are conducted on a computer with Intel® Core i7–8650 U CPU 1.9 GHz, 2.11 GHz, and 32 GB memory available. Our developed solution approach was implemented and run on Python 3.6 and applied IBM ILOG CPLEX Optimization Studio 12.7.

5.1. Parameter tuning and generation of new benchmark instances

We employed a systematic approach for parameter tuning, adhering to methodologies outlined in the literature (Ribeiro & Laporte, 2012; Jie et al., 2019). Ten instances from the new benchmarks underwent 10 runs per parameter value, exploring up to 10 values for each parameter (while keeping others constant). The value yielding the least average percent deviation from the best-found solution was selected as the optimal, and this process iterated until all parameters were tuned. Test values for some parameters were based on Hemmelmayr et al. (2012) and Jie et al. (2019), while others were determined through various experiments. The selected configuration and the range of tested values are detailed in Table 2.

The benchmark instances encompass ten sets categorized by the number of customers, spanning from 5 to 200 and classified as small (5–25 customers), medium (50 and 75 customers), and large (100–200 customers) size sets. The selected number of customers is aligned with established literature to cover a spectrum of small to large instances. To ensure both randomness and a realistic spatial distribution, customer locations are randomly chosen within a designated target zone. The zone's area varies, occupying 0.5 km^2 for instances with 5–25 customers, 1 km^2 for 50 customers, 5 km^2 for 75 customers, 10 km^2 for 100 customers, 15 km^2 for 150 customers, and 25 km^2 for 200 customers. The spatial grid, comprising 10x10 m cells, is employed for customer location selection, ensuring randomness to the extent that no two points can be selected from the same grid. Based on literature-derived insights, for small instances, the number of LEV depots is either 1 or 2, while medium and large instances have 3 or 4 depots. The number of transshipment points ranges from 2 to 4 in small instances and 5 to 10 in medium and large instances. Then, instances with IDs *SI-Dm-Cn-To, MI-Dm-Cn-To, and LI-Dm-Cn-To* represent respectively small, medium, and large size instances with *m* depots, *n* customers, and *o* transshipment points (tables 4 and 5).

Distances are transformed into travel time by considering speeds of 30 km/h for LEVs and 5 to 15 km/h for vessels traveling from the central hub to TPs. The unit energy consumption cost is 0.27 €/km for LEVs and ranges between 1.8 and 2.5 €/km for vessels. The period equivalent fixed cost of establishing transshipment points ranges from 100 to 175 €, based on the space of that TP.

Table 2
Applied parameter setting of the developed solution algorithm.

General		**Trial range (Min, Max)**
$\mathbb{T}_G$	50	(20,110)
$(\varrho_1, \varrho_2, \varrho_3, \varrho_4)$	(10,10,10,10)	((5,25),(5,25),(5,25),(5,25))
$(\varrho_1^{min}, \varrho_2^{min}, \varrho_3^{min}, \varrho_4^{min})$	(0.1,0.1,0.1,0.1)	((0.05,0.25),(0.05,0.25),(0.05,0.25),(0.05,0.25))
$(\varrho_1^{max}, \varrho_2^{max}, \varrho_3^{max}, \varrho_4^{max})$	(5000,5000,5000,5000)	((1k,10k),(1k,10k),(1k,10k),(1k,10k))
ψ_P	10	(5,35)
$\mathscr{L}^{\psi_P}$	$0.25 \times \psi_P$	$(0.05 \times \psi_P, 0.25 \times \psi_P)$
$(\omega_1, \omega_2, \omega_3)$	(1.2,1.2,1.2)	((0.5,1.4),(0.5,1.4),(0.5,1.4))
n	5	(2,8)
ALNS		
$\mathbb{T}_m$	2000	(500,2500)
$\mathbb{T}_{n-m}$	250	(50,350)
ψ_R	200	(50,300)
ψ_L	50	(10,100)
$[\Lambda_{min}, \Lambda_{max}]$	[0.05,0.15]	[(0.01,0.08),(0.05,0.5)]
$(\varpi_1, \varpi_2, \varpi_3)$	(6,4,5)	((1,10), (1,10), (1,10))
$\mathscr{J}$	50	(10,100)
θ	0.6	(0.1,0.9)

5.2. Experiment on existing benchmark instances

To assess the performance of our ALNS+*B*&P, we conduct experiments on well-known existing benchmark instances for 2E-VRP, two instance sets (sets 2 and 3) from Perboli et al. (2011) and one larger instance set (set 5) from Hemmelmayer et al. (2012). So, assumptions associated with locating TPs, electric vehicles, time windows, synchronization, and multiple delivery modes are relaxed. Therefore, our ALNS+*B*&P is decreased to solve a classic 2E-VRP. In Table (3), the performance of our algorithm on these benchmarks is compared with Hemmelmayer et al. (2012), Breunig et al. (2016); Enthoven et al. (2020), and Vincent et al. (2021).

The second column provides the Best-Known Solution (BKS) reported in Breunig et al. (2016). The next columns present the gap of the four papers' results to this BKS, and finally, we have the results of our proposed ALNS+*B*&P. The average run time and average gaps are reported in the last two rows of the table. It should be noted that these algorithms were run on different platforms, and our proposed solution approach is the only one among these four that incorporates an exact algorithm (B&P) in its structure. Accordingly, a precise comparison of time is not possible.

The average gap of our proposed approach is 0.14 % lower than Hemmelmayr et al. (2012), 0.21 % lower than Breunig et al. (2016), 0.37 % lower than Enthoven et al. (2020), and 0.38 % lower than Vincent et al. (2021). It should be noted that for sets 2 and 3, our results are almost identical to BKS. This is while for set 5, which embraces larger sizes, our proposed methodology improves BKS in six cases, with an average gap of -0.11 %. Considering these three sets of instances, our developed method provides better results than Hemmelmayr et al. (2012), Breunig et al. (2016), Enthoven et al. (2020), and Vincent et al. (2021) in 12, 13, 16, and 24 cases, respectively.

5.3. Experiment on newly generated benchmark instances

This section provides results on our newly generated benchmark instances. We first analyze the performance of our proposed algorithm on small-size instances. To this end, the results of the our algorithm are compared with the optimal (global or local) solutions provided by CPLEX.

Table (4) provides the results of our experiments on small-size instances. For CPLEX, the objective function value (Z_1) and run time (t) in seconds are reported. The computing time of CPLEX is limited by 2 h (7200 s). So, optimality is not guaranteed for instances that have reached this upper bound. In our proposed solution algorithm, Z_1 is associated with the best-found solution in ten runs of the algorithm. Δ_{CPLEX} represents the gap of the obtained objective function value to the one provided by CPLEX.

As Table (4) illustrates, our proposed solution algorithm establishes a good performance in solving small-size problems to optimality in a short time. In sets of 5, 10, and 15 customers, the optimality CPLEX results was guaranteed, and the computation time was shorter than two hours. Since the obtained gap is zero in these instances, our proposed algorithm's results are also globally optimum. In instances with 20 and 25 customers, CPLEX was unable to reach the global optimal within two hours. In these instances, the gap of CPLEX to the linear relaxation of the objective function found in iterations of branch and bound was less than 0.7 %. This implies that the obtained solutions by CPLEX were either globally optimal or very near to the global optimal. In these 12 instances, our solution algorithm achieved results equal to or smaller than those provided by CPLEX.

Table 3
The results of experiments on existing 2E-VRP benchmark instances.

Instance	BKS	Δ_{BKS}				
		Hemmelmayr et al. (2012)	Breunig et al. (2016)	Enthoven et al. (2020)	Vincent et al. (2021)	Our proposed approach
Set 2						
E-n22-k4-s6–17	417.07	0.00 %	0.00 %	0.00 %	0.00 %	0.00 %
E-n22-k4-s8–14	384.96	0.00 %	0.00 %	0.00 %	0.00 %	0.00 %
E-n22-k4-s9–19	470.6	0.00 %	0.00 %	0.00 %	0.00 %	0.00 %
E-n22-k4-s10–14	371.5	0.00 %	0.00 %	0.00 %	0.00 %	0.00 %
E-n22-k4-s11–12	427.22	0.00 %	0.00 %	0.00 %	0.00 %	0.00 %
E-n22-k4-s12–16	392.78	0.00 %	0.00 %	0.00 %	0.00 %	0.00 %
E-n33-k4-s1–9	730.16	0.00 %	0.00 %	0.00 %	0.00 %	0.00 %
E-n33-k4-s2–13	714.63	0.00 %	0.00 %	0.00 %	0.00 %	0.00 %
E-n33-k4-s3–17	707.48	0.00 %	0.00 %	0.00 %	0.00 %	0.00 %
E-n33-k4-s4–5	778.74	0.00 %	0.00 %	0.00 %	0.05 %	0.05 %
E-n33-k4-s7–25	756.85	0.00 %	0.00 %	0.00 %	0.00 %	0.00 %
E-n33-k4-s14–22	779.05	0.00 %	0.00 %	0.00 %	0.00 %	0.00 %
E-n51-k5-s2–17	597.49	0.00 %	0.00 %	0.00 %	0.00 %	0.00 %
E-n51-k5-s4–46	530.76	0.00 %	0.00 %	0.00 %	0.00 %	0.00 %
E-n51-k5-s6–12	554.81	0.00 %	0.00 %	0.00 %	0.04 %	0.00 %
E-n51-k5-s11–19	581.64	0.00 %	0.00 %	0.00 %	0.00 %	0.00 %
E-n51-k5-s27–47	538.22	0.00 %	0.00 %	0.00 %	0.00 %	0.00 %
E-n51-k5-s32–37	552.28	0.00 %	0.00 %	0.00 %	0.00 %	0.00 %
E-n51-k5-s2–4–17–46	530.76	0.00 %	0.00 %	0.00 %	0.00 %	0.00 %
E-n51-k5-s6–12–32–37	531.92	0.00 %	0.00 %	0.00 %	0.00 %	0.00 %
E-n51-k5-s11–19–27–47	527.63	0.00 %	0.00 %	0.00 %	0.00 %	0.00 %
Set 3						
E-n22-k4-s13–14	526.15	0.00 %	0.00 %	0.00 %	0.00 %	0.00 %
E-n22-k4-s13–16	521.09	0.00 %	0.00 %	0.00 %	0.00 %	0.00 %
E-n22-k4-s13–17	496.38	0.00 %	0.00 %	0.00 %	0.00 %	0.00 %
E-n22-k4-s14–19	498.8	0.00 %	0.00 %	0.00 %	0.00 %	0.00 %
E-n22-k4-s17–19	512.8	0.00 %	0.00 %	0.00 %	0.00 %	0.00 %
E-n22-k4-s19–21	520.42	0.00 %	0.00 %	0.00 %	0.00 %	0.00 %
E-n33-k4-s16–22	672.17	0.00 %	0.00 %	0.00 %	0.00 %	0.00 %
E-n33-k4-s16–24	666.02	0.00 %	0.00 %	0.00 %	0.00 %	0.00 %
E-n33-k4-s19–26	680.36	0.00 %	0.00 %	0.00 %	0.00 %	0.00 %
E-n33-k4-s22–26	680.36	0.00 %	0.00 %	0.00 %	0.00 %	0.00 %
E-n33-k4-s24–28	670.43	0.00 %	0.00 %	0.00 %	0.00 %	0.00 %
E-n33-k4-s25–28	650.58	0.00 %	0.00 %	0.00 %	0.00 %	0.00 %
E-n51-k5-s12–18	690.59	0.00 %	0.00 %	0.00 %	0.66 %	0.00 %
E-n51-k5-s12–41	683.05	0.00 %	0.00 %	0.00 %	1.70 %	0.00 %
E-n51-k5-s12–43	710.41	0.00 %	0.00 %	0.00 %	0.00 %	0.00 %
E-n51-k5-s39–41	728.54	0.00 %	0.00 %	0.00 %	0.00 %	0.00 %
E-n51-k5-s40–41	723.75	0.00 %	0.00 %	0.00 %	0.38 %	0.00 %
E-n51-k5-s40–43	752.15	0.00 %	0.00 %	0.00 %	0.26 %	0.00 %
Set 5						
100–5–1	1564.46	0.06 %	0.00 %	2.63 %	0.31 %	0.00 %
100–5–1b	1108.62	0.25 %	0.00 %	1.18 %	1.88 %	**-0.41** %
100–5–2	1016.32	0.00 %	0.00 %	0.57 %	0.50 %	0.00 %
100–5–2b	782.25	0.00 %	0.00 %	0.00 %	0.06 %	0.00 %
100–5–3	1045.29	0.00 %	0.00 %	0.07 %	0.05 %	0.00 %
100–5–3b	828.54	0.05 %	0.00 %	0.05 %	0.13 %	0.00 %
100–10–1	1124.93	0.47 %	0.05 %	0.01 %	0.02 %	0.00 %
100–10–1b	911.95*	0.49 %	0.46 %	1.01 %	1.36 %	**-0.02** %
100–10–2	990.58	0.00 %	2.18 %	2.03 %	2.57 %	0.00 %
100–10–2b	768.61	0.00 %	1.65 %	0.86 %	3.14 %	0.00 %
100–10–3	1043.25	0.00 %	0.62 %	0.94 %	0.63 %	0.00 %
100–10–3b	850.92	0.00 %	0.47 %	0.98 %	1.05 %	**-0.14** %
200–10–1	1549.07*	1.60 %	1.99 %	1.41 %	0.62 %	**-0.67** %
200–10–1b	1180.56*	1.77 %	0.92 %	1.22 %	0.68 %	**-0.39** %
200–10–2	1358.99*	1.15 %	0.54 %	2.19 %	2.41 %	0.49 %
200–10–2b	988.79*	1.49 %	1.95 %	1.38 %	0.42 %	0.40 %
200–10–3	1787.73	0.00 %	0.56 %	2.79 %	1.81 %	**-0.45** %
200–10–3b	1197.9	0.24 %	0.36 %	1.84 %	0.95 %	0.00 %
Avg. Gap		0.133 %	0.206 %	0.371 %	0.380 %	-0.003 %
Avg. Time (min)		4.31	5.67	5.71	4.76	6.48

* BKS reported by Huang et al. (2021).

Table (5) presents the result of investigating the performance of our proposed algorithm that applies ALNS, hybridized with K-means and LS, together with B&P on benchmark instances of 50–200 customers. To this end, the objective function value of the best known solution (BKS), which is found during the overall testing of the algorithm, is reported. Then, the performance of the proposed algorithm with and without its hybridization with K-means and LS is investigated, and related results, associated with the best solution of ten runs, including the objective

Table 4
The results of experiments on newly generated small-size benchmark instances.

Instance	CPLEX		Proposed solution algorithm		
	Z_1	t (s)	Z_1	Δ_{CPLEX}	t (s)
SI-D1-C5-T2	119.5287	1.06	119.5287	0.000 %	5.28
SI-D2-C5-T2	119.4544	1.17	119.4544	0.000 %	5.32
SI-D1-C5-T3	119.3063	1.16	119.3063	0.000 %	5.28
SI-D2-C5-T3	119.4544	1.19	119.4544	0.000 %	5.64
SI-D1-C5-T4	119.3063	1.18	119.3063	0.000 %	7.12
SI-D2-C5-T4	119.4544	1.26	119.4544	0.000 %	6.44
SI-D1-C10-T2	119.9658	2.42	119.9658	0.000 %	11.43
SI-D2-C10-T2	120.1536	1.97	120.1536	0.000 %	14.02
SI-D1-C10-T3	119.9658	2.64	119.9658	0.000 %	11.69
SI-D2-C10-T3	120.1536	2.73	120.1536	0.000 %	13.23
SI-D1-C10-T4	119.9658	2.81	119.9658	0.000 %	12.01
SI-D2-C10-T4	120.1536	2.75	120.1536	0.000 %	15.87
SI-D1-C15-T2	286.1563	43.16	286.1563	0.000 %	31.34
SI-D2-C15-T2	286.1212	52.84	286.2178	0.034 %	28.82
SI-D1-C15-T3	231.3617	54.25	231.3617	0.000 %	32.53
SI-D2-C15-T3	230.9398	580.52	230.9398	0.000 %	35.72
SI-D1-C15-T4	231.3617	675.63	231.3617	0.000 %	34.03
SI-D2-C15-T4	230.9398	652.23	230.9398	0.000 %	37.45
SI-D1-C20-T2	295.9807	7200	295.9807	0.000 %	88.74
SI-D2-C20-T2	295.7998	7200	295.7854	-0.005 %	84.67
SI-D1-C20-T3	296.8966	7200	296.7154	-0.061 %	95.62
SI-D2-C20-T3	296.9625	7200	296.8275	-0.045 %	105.35
SI-D1-C20-T4	296.7437	7200	296.7154	-0.010 %	82.38
SI-D2-C20-T4	296.8345	7200	296.8275	-0.002 %	104.95
SI-D1-C25-T2	298.0373	7200	297.5612	-0.160 %	137.42
SI-D2-C25-T2	299.1454	7200	297.5629	-0.434 %	121.06
SI-D1-C25-T3	299.3157	7200	298.2126	-0.369 %	132.14
SI-D2-C25-T3	298.8595	7200	298.0089	-0.285 %	130.01
SI-D1-C25-T4	298.3536	7200	298.2126	-0.047 %	141.77
SI-D2-C25-T4	298.5121	7200	298.3093	-0.068 %	162.82
Avg.		2949.36		-0.048 %	56.67

function value (Z_1), its gap to BKS (Δ_{BKS}), and run time (t), are reported.

The observed results indicate that the intensified algorithm, which incorporates local search and K-means clustering in addition to adaptive large neighborhood search and branch and price, consistently outperforms the alternative algorithm in terms of solution quality. The average gap with the best-known solution (BKS) is approximately 3.5 % lower for the intensified algorithm. Although the intensified algorithm requires an average execution time that is 1.5 min longer, the inclusion of K-means clustering helps mitigate this increase, resulting in a reasonably close execution time to the alternative algorithm. Moreover, as the size of the problem instances grows, it is unsurprising that the gaps widen, given the increased difficulty in finding high-quality solutions. Simultaneously, the enhanced algorithm demonstrates a more pronounced performance advantage. This suggests that the additional time taken by the local search component is worthwhile, as it contributes to improved solutions for larger problem instances.

5.4. Case study

This section provides an optimal design for the distribution chain of restaurants and cafés located in Amsterdam's historical center. Amsterdam's city center is a well-known hub, with many hotels, restaurants, and cafés tightly clustered together. More than 1500 HoReCa spots exist in this area, requiring a huge distribution chain for their input food supplies. The location of restaurants and cafés is derived from the municipality of Amsterdam's provided maps.[4] The municipality has also specified a set of potential locations for TPs classifying them into poor, moderate, and spacious. Fig. (3) illustrates the location of these TPs, together with restaurants and cafés.

To estimate the daily demand of these businesses (in m^3), we have incorporated a Deep Neural Network (DNN), featuring two hidden layers with a rectified linear unit (ReLU) activation function. This DNN leverages five input labels: business type (restaurant or café), weekday or weekend, season (spring, summer, autumn, winter), longitude, and latitude. To represent the input for the first three labels, we utilize binary sub-labels (for example, the business type is designated as 'restaurant' when the corresponding sub-label is 1, and 'café' when it is 0). Our input demand data is partitioned into 70 % training and 30 % validation data, collected through field trips.

We initially clustered the city center into five location groups based on the longitude and latitude of existing restaurants and cafés, and within each cluster, a number of restaurants and cafés was selected as visiting candidates for field trip. This approach ensures that our candidates were geographically diverse, offering a representation of the entire area. The number of visits within each cluster was proportional to the number of all existing restaurants and cafés (based on intensity varying between 12 %-20 %), leading to a total of 259 visits. The data from 17 visits were excluded from our analysis due to unclear or incomplete responses. In each visit, a structured interview was conducted to get the volume of demanded food supply, during weekend and weekdays and concerning four seasons (providing us with 8 demand data for each visit).The other input parameters are specified in consultation with experts in the area and are identical to the ones introduced in Section 5.1. Furthermore, the average weight of an LEV is considered as 700 kg, applied trucks vary between 2000 and 3500 kg. The average emission per 1000 kg per travelled distance of a diesel truck is considered as 52.7 gr (Leirião et al., 2020).

Fig. (4) Illustrates the result of solving the problem for the case of Amsterdam.

While literature often deals with up to 200 customers, our algorithm excels in scalability, handling up to 1500 demand points effectively. The results of our case study, as depicted in Fig. (4), illustrates the establishment of 10 transshipment locations (TPs) strategically positioned within the city center, with a focus on densely populated areas. The majority are categorized as moderate, with one spacious and two considered poor in size and capacity. Map examination shows that potential spacious TPs avoid densely populated segments, justifying their absence. Poor TPs are established only where spacious or moderate alternatives are lacking. Considering the integration of TPs with existing infrastructure, challenges vary by TP category. Spacious TPs, benefiting from well-prepared infrastructure, seamlessly integrate with minimal disruptions. In contrast, poor TPs pose intricate challenges, requiring careful replacement and adjustment of existing infrastructure. Moderate TPs present a middle ground, demanding a balanced approach to integration efforts. This categorization provides insights into the practical implementation of the new system within the urban infrastructure.

To efficiently cater to the demands, a fleet of seven small and two medium vessels is employed, without the inclusion of any large vessels. Despite the potential cost-saving benefits, the use of large vessels was not feasible concerning the canal classes due to the limited width or depth of the canals within the city center. In the second echelon of our proposed system, 74 LEVs and 133 Moving Jacks are utilized to deliver the items to their final destinations. This indicates the appropriate location of established TPs has effectively reduced the number of LEVs required, thanks to the inclusion of Moving Jacks for serving points that are in close proximity to waterways.

A fundamental question in evaluating the efficiency of this waterway-based chain is if it can improve the distribution of the HoReCa demands. In order to answer this question, we compare the designed distribution chain with the one currently implemented in Amsterdam, for which trucks with a weight limit of 3500 kg deliver the items to demanded spots. This transforms the problem into a routing problem with time windows. Fig. (5) compares these two distribution chains in terms of the total cost, the total number of applied road vehicles, their

[4] Available at https://maps.amsterdam.nl/functiekaart/

Table 5
The results of experiments on newly generated medium and large-size benchmark instances.

Instance	BKS	ALNS+*B&P*(+ *K*-means +*LS*)			ALNS+*B&P*		
		Z_1	Δ_{BKS}	t (m)	Z_1	Δ_{BKS}	t (m)
MI-D3-C50-T5	395.9445	395.9445	0.000 %	5.36	396.8985	0.241 %	4.98
MI-D4-C50-T5	394.9225	394.9225	0.000 %	5.88	396.3533	0.362 %	5.35
MI-D3-C50-T10	369.9841	369.9841	0.000 %	5.64	371.8903	0.515 %	5.19
MI-D4-C50-T10	368.2105	368.4828	0.074 %	6.12	370.1435	0.525 %	5.81
MI-D3-C75-T5	437.5509	437.5509	0.000 %	8.18	446.5644	2.056 %	6.47
MI-D4-C75-T5	435.0217	435.3131	0.067 %	9.27	447.6808	2.913 %	7.21
MI-D3-C75-T10	398.1412	398.4636	0.081 %	8.71	410.2845	3.048 %	6.95
MI-D4-C75-T10	396.8405	397.2135	0.094 %	9.43	409.6187	3.215 %	7.89
LI-D3-C100-T5	498.3201	498.8184	0.102 %	11.32	514.4656	3.235 %	9.62
LI-D4-C100-T5	492.0076	492.5981	0.117 %	11.69	510.7531	3.812 %	10.05
LI-D3-C100-T10	471.0568	471.5749	0.105 %	11.61	489.9461	4.007 %	9.75
LI-D4-C100-T10	468.1005	468.6622	0.122 %	12.05	487.3862	4.116 %	10.12
LI-D3-C150-T5	614.2237	615.4275	0.196 %	15.21	641.9374	4.512 %	12.01
LI-D4-C150-T5	601.5589	602.7561	0.199 %	15.33	628.2801	4.442 %	12.55
LI-D3-C150-T10	583.0153	584.1171	0.189 %	15.12	610.5394	4.721 %	12.84
LI-D4-C150-T10	580.1116	581.2892	0.203 %	15.56	608.5892	4.909 %	13.09
LI-D3-C200-T5	807.4012	809.5891	0.271 %	18.42	858.4045	6.317 %	16.35
LI-D4-C200-T5	804.3613	806.5006	0.266 %	18.87	856.8133	6.521 %	16.58
LI-D3-C200-T10	785.0109	787.0264	0.257 %	18.59	835.5792	6.442 %	16.49
LI-D4-C200-T10	783.0784	785.0591	0.253 %	19.01	833.5943	6.451 %	16.73
Avg.			0.131 %	12.07		3.618 %	10.31

associated weight, and the average distance driven by each vehicle within the city center.

The analysis reveals that the waterway-based food distribution chain presents a noteworthy advantage in terms of total cost, leading to cost savings of approximately 28 % compared to the truck-based system. Despite the higher number of vehicles employed in the bi-modal setting, it is important to note that these vehicles are light vehicles (on average, each LEV weighs 20–28 % of the utilized trucks), resulting in a 43 % reduction in the total weight of vehicles driven within the city center. This not only offers the potential to preserve the lifetime of physical infrastructure such as quay walls and bridges but also indicates a more distributed and flexible delivery system.

Moreover, the waterway-based food chain demonstrates a significant 80 % reduction in the average distance driven within the city center to serve the HoReCa spots compared to the truck-based system. This reduction in distance traveled has the potential to alleviate traffic congestion, improve efficiency in terms of time and fuel consumption, and contribute to decreased emissions. Moreover, the bi-modal setting,

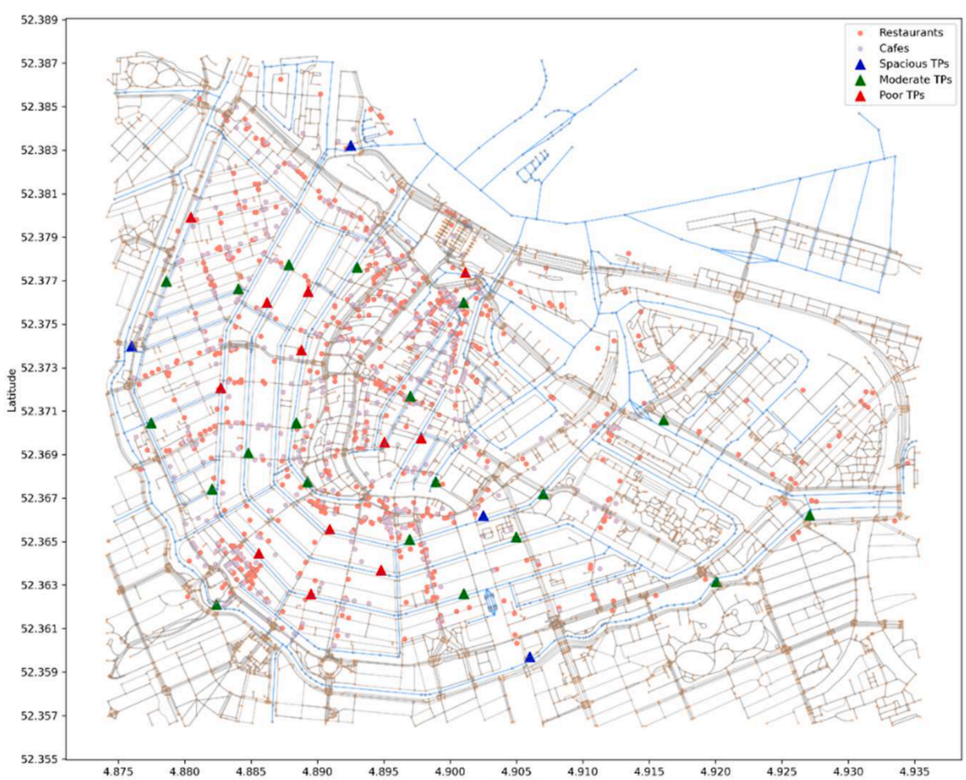

Fig. 3. Restaurants and Cafés in the city center of Amsterdam.

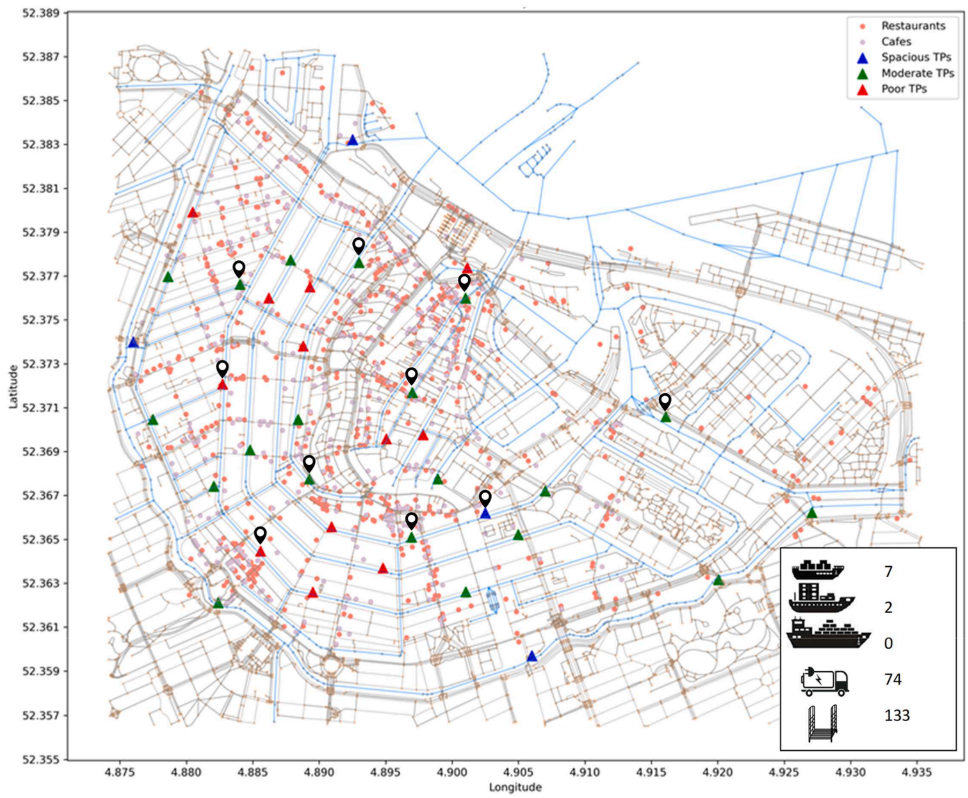

Fig. 4. Case study results.

incorporating LEVs and electric vessels, yields a significant reduction in carbon emissions (43.46 kg daily) compared to the truck-based setting.

In conclusion, the results suggest that implementing the waterway-based distribution chain has the potential to enhance the efficiency of HoReCa demands in Amsterdam. The advantages encompass lower total cost, a more distributed fleet of lighter vehicles, a significant reduction in average distance driven within the city center, and a notable decrease in exhaust emissions.

5.5. Sensitivity analysis

In this sub-section, we investigate the impact of different input parameters on our designed network. To track this impact on all decision variables, a medium instance with three depots, five transshipment

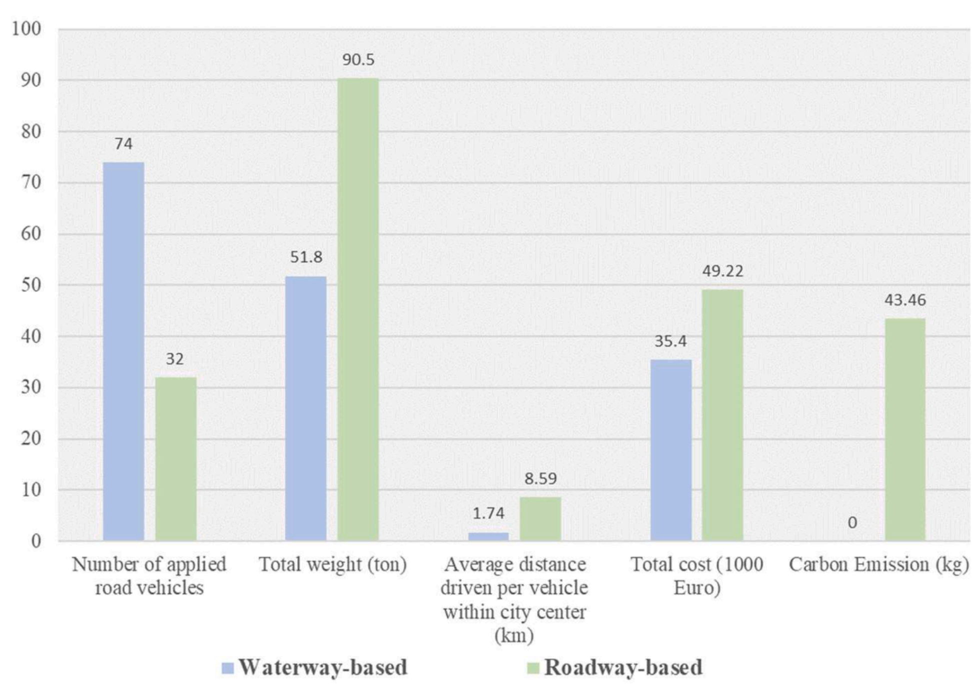

Fig. 5. Comparison between waterway-based and roadway-based logistics chain.

Table 6
The impact of changes on different cost parameters.

Parameter	Changes (%)	Total Cost	n_{TP}	n_V	n_{LEV}
	-75 %	129.85	5	3	21
	-50 %	230.55	5	3	21
	-25 %	308.07	4	3	26
FC_i	0	395.94	4	3	26
	+25 %	486.24	4	3	26
	+50 %	575.24	3	3	32
	+75 %	664.24	3	3	32
	-75 %	362.54	4	4	27
	-50 %	379.88	4	3	26
	-25 %	391.51	4	3	26
C^I_{ijk}	0	395.94	4	3	26
	+25 %	405.51	4	3	26
	+50 %	414.54	4	3	26
	+75 %	442.38	4	3	26
	-75 %	390.99	4	3	28
	-50 %	392.64	4	3	27
	-25 %	394.29	4	3	27
C^{II}_{ijk}	0	395.94	4	3	26
	+25 %	397.59	4	3	26
	+50 %	399.23	4	3	26
	+75 %	400.89	4	3	25

locations, and 50 customers is selected. The parameters associated with the period equivalent establishment cost and travel cost are the two cost factors characterizing the economic competency of our designed waterway-based distribution chain. In order to investigate their impact on total cost, number of established TPs, number of applied vessels, and number of applied LEVs, sensitivity analyses are carried out on these parameters, and the results are provided in Table (6).

The results indicate that changes in transshipment location establishment costs have a significantly larger influence on total costs compared to variations in first and second echelon transportation costs. Specifically, by reducing the establishment costs, the number of established locations may increase, leading to a decreased reliance on LEVs for transportation. This reduction in LEV usage was attributed to the improved efficiency achieved through the utilization of Moving Jacks for item delivery. This highlights that by efficiently reducing this cost, one not only achieves cost savings but also contributes to a reduction in road traffic volume through fewer applied vehicles. This emphasis specifically centers on the number of applied vehicles, representing a subset of the broader traffic network. Conversely, the variations in first and, specifically, second echelon transportation costs were found to have a relatively minor impact on overall costs. These findings underscore the importance of effectively managing and optimizing transshipment location establishment costs as a key strategy for achieving cost efficiencies in transportation operations, while lower attention can be devoted to the second echelon transportation.

6. Discussion

The analysis results are compelling, revealing substantial benefits. Implementing the waterway-based distribution chain led to significant cost savings (28 %) compared to the truck-based system. Utilizing lighter vehicles reduced the total weight in the city center by 43 %. The waterway-based system achieved an impressive 80 % reduction in average travel distance, promising relief from traffic congestion and improved efficiency. Additionally, the adoption of electric vehicles in the bi-modal setting cut daily carbon emissions by 43.46 kg, further underscoring the environmental advantages of this distribution chain. Our sensitivity analysis emphasizes the critical role of optimizing transshipment location establishment costs for efficient transportation operations. Reducing these costs not only results in overall savings but also diminishes reliance on LEVs and alleviates road traffic congestion. Prioritizing the optimization of transshipment location establishment costs emerges as a key strategy for achieving cost efficiency, surpassing the relatively minor impact of first and second echelon transportation costs.

While Amsterdam serves as the focal point of our case study, our model and solution approach hold broader applicability across diverse urban environments and logistical contexts characterized by rich inland waterways. The challenges confronted by Amsterdam, congestion, emission, and strained infrastructure, mirror issues encountered by numerous cities undergoing rapid urbanization. The demonstrated effectiveness of our algorithm and the proven advantages of a waterway-based distribution chain offer a promising blueprint for cities globally wrestling with analogous challenges.

The envisioned modal shift, despite its potential advantages, poses multifaceted challenges. Political obstacles may emerge due to necessary policy adjustments and resource reallocation. Logistically, adapting infrastructure and establishing transshipment points may encounter difficulties, particularly in densely populated or historically significant zones. Successful implementation hinges on garnering societal acceptance through effective communication and outreach initiatives. Addressing these challenges is crucial for unlocking the full potential of the waterway-based distribution chain and ensuring its smooth integration into the urban logistics landscape.

The study's findings carry significant implications for urban policy and transportation planning, both in Amsterdam and beyond. The establishment of a waterway-based distribution chain, with its reduced distance traveled and a distributed fleet of smaller vehicles, presents a more flexible and adaptable delivery system that can be of particular interest to city authorities and policymakers. Integrating urban waterways into the transportation network not only brings various benefits but also extends the lifespan of historical heritage, making it particularly appealing to municipalities and society. Policymakers are encouraged to incentivize the adoption of electric vehicles in logistics operations, aligning with broader environmental sustainability objectives. Moreover, strategic planning for transshipment locations, with an emphasis on cost optimization, becomes crucial for policymakers aiming to enhance overall system efficiency. These provide actionable insights for policymakers to embrace innovative strategies in urban logistics, contributing to sustainable transportation practices and enhancing the urban living experience.

7. Conclusion

This study proposes an efficient urban logistics solution for Amsterdam, integrating urban waterways and last-mile delivery. It emphasizes the untapped potential of inland waterways to address logistical challenges, offering a two-echelon location routing problem with time windows and a hybrid solution approach.

The proposed algorithm consistently outperforms existing methods, showcasing its effectiveness across established benchmarks and new instances. In a comprehensive case study, the waterway-based distribution chain demonstrated noteworthy advantages, including a 28 % cost savings compared to traditional truck-based systems. The adoption of lighter vehicles resulted in a 43 % reduction in total vehicle weight within the city center, promoting infrastructure longevity and a more flexible delivery system. Furthermore, the waterway-based chain achieved an impressive 80 % reduction in average travel distance, offering potential relief from traffic congestion, enhanced efficiency. Incorporating electric vehicles further contributed to reduced carbon emissions, underscoring the environmental benefits. The sensitivity analysis highlighted the crucial role of optimizing transshipment location establishment costs for overall cost efficiencies, providing valuable insights for cities worldwide seeking sustainable solutions in urban logistics.

Limitations and future research

While our study offers valuable insights for promoting sustainable transportation practices, it is essential to address its inherent limitations. A part of numerical analysis relies on newly developed benchmark instances, introducing potential biases despite our randomized approach. It is strongly recommended to enhance the research by incorporating further benchmark instances and exploring various logistical settings. While existing literature typically deals with up to 200 customer locations, our algorithm demonstrates scalability, effectively handling up to 1500 demand points in our case study. However, further investigation into its performance with even larger instances is suggested to reflect cities with different settings and dimensions.

The strategic decision of locating transshipment points (TPs) is based on average demand, where small variations have minimal impact. However, routing decisions can be significantly affected by demand fluctuations and congestion patterns. Therefore, addressing uncertainty becomes crucial for comprehensive optimization.

Despite the efficiency of optimization models, they inherently fall short in fully accounting for detailed and dynamic traffic and infrastructure features. A comprehensive analysis is needed to assess the viability and potential benefits of implementing the waterway-based chain, considering infrastructural limitations and canal features. The impact of a modal shift on water traffic and the potential increase in propeller wash, leading to further deterioration of bed levels and quay walls, requires thorough examination. To facilitate this, the development of a digital twin for Amsterdam's city center canals is proposed. This digital twin would illustrate the consequences of network design changes, establishing a feedback loop between optimization and simulation for improved insights and scenario analysis. This innovative approach allows leveraging the design capability of optimization while exploring specific solution space directions, offering a holistic perspective on the proposed waterway-based distribution chain.

CRediT authorship contribution statement

Nadia Pourmohammad-Zia: Writing – review & editing, Writing – original draft, Visualization, Validation, Software, Resources, Project administration, Methodology, Investigation, Formal analysis, Data curation, Conceptualization. **Mark van Koningsveld:** Writing – review & editing, Supervision, Conceptualization.

Declaration of competing interest

Authors hereby confirm that there exists no declaration of interest.

Data availability

Data will be made available on request.

Acknowledgement

The authors extend their appreciation to the Amsterdam Institute for Advanced Metropolitan Solutions (AMS) for the collaboration and support throughout this research. Their partnership has been instrumental, enriching our insights and collective understanding of the subject matter.

Appendix A. In-Depth Exploration of Mathematical Equations

$$\boldsymbol{P}_1 : \min \boldsymbol{Z} = \sum_{k\in K_1}\sum_{i\in V_1}\sum_{j\in V_1} \boldsymbol{C}^{I}_{ijk}\boldsymbol{x}^{I}_{ijk} + \sum_{k\in K_2}\sum_{i\in V_2}\sum_{j\in V_2} \boldsymbol{C}^{II}_{ijk}\ \boldsymbol{x}^{II}_{ijk} + \sum_{i\in TP} \boldsymbol{FC}_i\ \boldsymbol{y}_i \tag{A1}$$

The objective function minimizes the total cost, including the travel cost of the vehicles in the first and second echelons and the period equivalent establishment cost of transshipment points.

$$\sum_{j\in TP} x^{I}_{ijk} \le 1 \qquad \forall i \in \{CH\},\ k \in K_1 \tag{A2}$$

Each vessel leaves the central hub at most once (The maximum number of times each vessel can originate from the central hub and transit to one of the TPs, is one).

$$\sum_{i\in V_1} x^{I}_{ivk} - \sum_{j\in V_1} x^{I}_{vjk} = 0 \qquad \forall v \in TP,\ k \in K_1 \tag{A3}$$

These are flow constraints in the first echelon (If a vessel enters a TP, it should also leave that TP).

$$\sum_{i\in V_1} x^{I}_{ijk} \le y_j \qquad \forall j \in TP,\ k \in K_1 \tag{A4}$$

A TP can only be visited by a vessel if that point is established (If the TP is not established ($y_j = 0$), no vessel can enter that location).

$$at^{I}_{jk} = \sum_{i\in V_1}\left(st^{I}_{ik} + S^{I}_{i} + T^{I}_{ijk}\right)x^{I}_{ijk} \qquad \forall j \in V_1,\ k \in K_1 \tag{A5}$$

These show vessels' arrival time consistency at a node (A vessel is expected to arrive at a node immediately after completing its service at the preceding node and traveling from that node to the current one).

$$st^{I}_{ik} \ge at^{I}_{ik} \qquad \forall i \in V_1,\ k \in K_1 \tag{A6}$$

The service at a node can start after the vessel arrives at that node (The consistency of service time at a node).

$$st^{I}_{ik} + S^{I}_{i} - at^{I}_{ik} \le AL_i \qquad \forall i \in TP,\ k \in K_1 \tag{A7}$$

The duration of a vessel's stay at a TP, the period from its arrival to its departure, cannot exceed the admissible laying time of that TP.

$$\sum_{i\in TP} q_{ik} \le Q^{I}_{k} \qquad \forall k \in K_1 \tag{A8}$$

These show the capacity limits of each vessel (The total volume delivered by a vessel to all TPs collectively cannot exceed the designated capacity of that vessel).

$$q_{jk} \leq M_1 \sum_{i \in V_1} x^{I}_{ijk}$$

$$\forall j \in TP,\ k \in K_1 \quad \text{(A9)}$$

The delivery volume of a vessel to a is only permitted to be non-zero if the vessel actually enters the specified TP (The constraints enforce a direct correlation between vessel entry into a TP and the associated delivery volume).

$$q_{ik} = \sum_{j \in HRC} D_j\ p_{ijk}$$

$$\forall i \in TP,\ k \in K_1 \quad \text{(A10)}$$

The quantity a vessel delivers to a TP should satisfy the collective demands of the HoReCa businesses designated to be served by that specific vessel at the given TP.

$$\sum_{k \in K_1} \sum_{i \in TP} p_{ijk} = 1 \qquad \forall j \in HRC \quad \text{(A11)}$$

Each demand point must be exclusively serviced by one vessel and one TP (The items demanded by a HoReCa business cannot be delivered by more than one vessel, nor can they be distributed across multiple TPs).

$$p_{ijk} \leq \sum_{\upsilon \in V_1} x^{I}_{\upsilon ik} \qquad \forall i \in TP,\ k \in K_1 \quad \text{(A12)}$$

A specific vessel in conjunction with a specific TP can serve a demand point only if the vessel visits that TP (The allocation of vessels to demand points is contingent upon the vessels' presence at the respective TPs).

$$\sum_{k \in K_1} \sum_{j \in HRC} D_j\ \ p_{ijk} \leq CAP_i \qquad \forall i \in TP \quad \text{(A13)}$$

These conditions define the capacity limits of TPs (The maximum volume a TP can allocate to different demand points is equal to its designated capacity).

$$DTr - DIS_{ij} \leq M_2 l_{ij} \qquad \forall i \in TP, j \in HRC \quad \text{(A14)}$$

$$DTr - DIS_{ij} \geq m_1 \left(1 - l_{ij}\right) \qquad \forall i \in TP, j \in HRC \quad \text{(A15)}$$

The auxiliary parameter l_{ij} takes the value of one only if the distance between its showcased TP and demand point is less than the predefined threshold: If the left-side is a negative value, indicating that the distance is more than the threshold, l_{ij} has to be zero according to constraints (A15). On the contrary, if the left-side is a positive value, i.e. the distance is less than the threshold, l_{ij} has to be one according to constraints (A14).

$$\sum_{k \in K_1} p_{ijk} + l_{ij} \leq 1 + u_{ij} \qquad \forall i \in TP, j \in HRC \quad \text{(A16)}$$

$$\sum_{k \in K_1} p_{ijk} + l_{ij} \geq 2u_{ij} \qquad \forall i \in TP, j \in HRC \quad \text{(A17)}$$

If a demand point is allocated to a specific TP, and its distance from that TP is less than the pre-specified threshold, that demand point will be served by a Moving Jack: If either of the two left-side values is zero, u_{ij} must be zero according to constraints (A17). On the contrary, if both of the two left-side values are one, u_{ij} has to be one according to constraints (A16).

$$\sum_{i \in VD} \sum_{j \in V_2} x^{II}_{ijk} \leq 1$$

$$k \in K_2 \quad \text{(A18)}$$

Each LEV can leave one of the vehicle depots and at most once (The maximum number of times each LEV originates from all depots to all TPs collectively cannot exceed one).

$$\sum_{i \in V_2} x^{II}_{ijk} \leq y_j$$

$$\forall j \in TP,\ k \in K_2 \quad \text{(A19)}$$

A transshipment location can only be visited by an LEV if that point is established (If the TP is not established ($y_j = 0$), no LEV can enter that location).

$$\sum_{i \in V_2} x^{II}_{i\upsilon k} - \sum_{i \in V_2} x^{II}_{\upsilon jk} = 0$$

$$\forall \upsilon \in TP \cup HRC,\ k \in K_2 \quad \text{(A20)}$$

These are flow constraints in the second echelon (if an LEV enters a point, TP or demand point, it should also leave that point).

$$\sum_{k \in K_2} \sum_{i \in V_2} x^{II}_{ijk} + \sum_{i \in V_2} u_{ij} = 1$$

$$\forall j \in HRC \quad \text{(A21)}$$

Each demand point is served either by an LEV or a Moving Jack (either an LEV or a Moving Jack will visit a demand point).

$$\sum_{i\in V_2}\sum_{j\in V_2} DIS^{I}_{ijk}\ x^{I}_{ijk} \le DL^{I}_{k}$$

$$\forall k \in K_1 \tag{A22}$$

These show the limited shipping range of vessels (The maximum travelled distance of a vessel is limited by its driving range).

$$\sum_{i\in V_2}\sum_{j\in V_2} DIS^{II}_{ij}\ x^{II}_{ijk} \le DL^{II}$$

$$\forall k \in K_2 \tag{A23}$$

These show the limited driving range of LEVs (The maximum travelled distance of an LEV is limited by its driving range).

$$\sum_{i\in V_2}\sum_{j\in V_2} D_j\ \ x^{II}_{ijk} \le Q^{II}_{k}$$

$$\forall k \in K_2 \tag{A24}$$

These show the capacity limits of each LEV (The total volume delivered by an LEV to all demand points collectively cannot exceed the designated capacity of that LEV).

$$st^{II}_{ik} \ge \left(st^{II}_{ik} + S^{II}_{i} + T^{II}_{ijk}\right)x^{II}_{ijk}$$

$$\forall i,j \in V_2,\ k \in K_2 \tag{A25}$$

These show LEVs' service time consistency at a node (An LEV starts serving a node after completing its service at the preceding node and traveling from that node to the current one).

$$st^{III}_{jj} = \left(st^{III}_{ij} + S^{II}_{i} + T^{III}_{ij}\right)u_{ij}$$

$$\forall i \in TP, j \in HRC \tag{A26}$$

These show Moving Jacks' service time consistency at a node (A Moving Jack is expected to start serving a demand node immediately after completing its service at the TP and traveling from that TP to the current node).

$$st^{II}_{i\hat{k}} - st^{I}_{ik} - S^{I}_{i} \ge m_2(1 - v_{k\hat{k}i})$$

$$\forall i \in TP,\ k \in K_1, \hat{k} \in K_2 \tag{A27}$$

When a vessel and an LEV are synchronized, their service time should be consistent (An LEV is expected to start loading process at a TP, after its synchronized vessel serves that TP).

$$st^{III}_{ij} - st^{I}_{ik} - S^{I}_{i} \ge m_3\left(1 - pu_{ijk}\right)$$

$$\forall i \in TP, j \in HRC,\ k \in K_1 \tag{A28}$$

When a vessel and a Moving Jack are synchronized, their service time should be consistent (A Moving Jack can start loading process at a TP, after its synchronized vessel serves that TP).

$$p_{ijk} + u_{ij} \le 1 + pu_{ijk}$$

$$\forall i \in TP, j \in HRC,\ k \in K_1 \tag{A29}$$

$$p_{ijk} + u_{ij} \ge 2pu_{ijk}$$

$$\forall i \in TP, j \in HRC,\ k \in K_1 \tag{A30}$$

A vessel and a Moving Jack at a TP are considered synchronized only when the demand point to be served by the Moving Jack is allocated to the same vessel at that specific TP.

$$v_{k\hat{k}j} \le \sum_{i\in V_1} x^{I}_{ijk}$$

$$\forall j \in TP,\ k \in K_1, \hat{k} \in K_2 \tag{A31}$$

A vessel and an LEV can be synchronized at a TP, only if that particular vessel visits the mentioned TP.

$$\sum_{k\in K_1} v_{k\hat{k}i} = \sum_{j\in V_2} x^{II}_{ij\hat{k}}$$

$$\forall i \in TP,\ \hat{k} \in K_2 \tag{A32}$$

An LEV will be synchronized by one of the vessels at a TP, only if that particular LEV visits the mentioned TP.

$$\sum_{k\in K_1}\sum_{i\in TP} v_{k\hat{k}i} \leq 1$$

$\forall \hat{k} \in K_2$ (A33)

An LEV is synchronized at most by one vessel and at one TP.

$$\sum_{\hat{k}\in K_2} v_{k\hat{k}i} + pu_{ijk} \geq p_{ijk}$$

$\forall i \in TP, j \in HRC,\ k \in K_1$ (A34)

If a demand point is designated to be served by a vessel from a specific TP, there must be at least one synchronization event involving that vessel at the specified TP, either with a Moving Jack or an LEV.

$$TA_j \sum_{i\in V_2} x^{II}_{ijk} \leq st^{II}_{jk} \leq TB_j \sum_{i\in V_2} x^{II}_{ijk}$$

$\forall j \in \mathrm{HRC},\ k \in K_2$ (A35)

The service time of demand points can only start within admissible time windows (LEVs).

$$TA_j \sum_{i\in TP} u_{ij} \leq st^{III}_{jj} \leq TB_j \sum_{i\in TP} u_{ij}$$

$\forall j \in \mathrm{HRC}$ (A36)

The service time of demand points can only start within admissible time windows (Moving Jacks).

$$x^{I}_{ijk}, x^{II}_{ijk},\ y_i,\ p_{ijk},\ v_{k\hat{k}i}, u_{ij},\ pu_{ijk}\ \in \{0,1\}$$

$\forall i,j \in V,\ k \in K$ (A37)

The binary variables

$$st^{I}_{ik}, st^{II}_{ik}, st^{III}_{i},\ q_{ik} \geq 0$$

$\forall i,j \in V,\ k \in K$ (A38)

The non-zero continuous variables

References

Akbay, M. A., Kalayci, C. B., Blum, C., & Polat, O. (2022). Variable neighborhood search for the two-Echelon electric vehicle routing problem with time windows. *Applied Sciences, 12*(3), 1014.

Akpunar, Ö.Ş., & Akpinar, Ş. (2021). A hybrid adaptive large neighbourhood search algorithm for the capacitated location routing problem. *Expert Systems with Applications, 168*, 114304.

Aloui, A., Hamani, N., & Delahoche, L. (2021). An integrated optimization approach using a collaborative strategy for sustainable cities freight transportation: A Case study. *Sustainable Cities and Society, 75*, Article 103331.

Anderluh, A., Nolz, P. C., Hemmelmayr, V. C., & Crainic, T. G. (2021). Multi-objective optimization of a two-echelon vehicle routing problem with vehicle synchronization and 'grey zone'customers arising in urban logistics. *European Journal of Operational Research, 289*(3), 940–958.

Barnhart, C., Johnson, E. L., Nemhauser, G. L., Savelsbergh, M. W., & Vance, P. H. (1998). Branch-and-price: Column generation for solving huge integer programs. *Operations research, 46*, 316–329.

Barreto, S., Ferreira, C., Paixao, J., & Santos, B. S. (2007). Using clustering analysis in a capacitated location-routing problem. *European Journal of Operational Research, 179* (3), 968–977.

Belgin, O., Karaoglan, I., & Altiparmak, F. (2018). Two-echelon vehicle routing problem with simultaneous pick-up and delivery: Mathematical model and heuristic approach. *Computers & Industrial Engineering, 115*, 1–16.

Bevilaqua, A., Bevilaqua, D., & Yamanaka, K. (2019). Parallel island based memetic algorithm with Lin–Kernighan local search for a real-life two-echelon heterogeneous vehicle routing problem based on Brazilian wholesale companies. *Applied Soft Computing, 76*, 697–711.

Breunig, U., Schmid, V., Hartl, R. F., & Vidal, T. (2016). A large neighbourhood based heuristic for two-echelon routing problems. *Computers & Operations Research, 76*, 208–225.

Breunig, U., Baldacci, R., Hartl, R. F., & Vidal, T. (2019). The electric two-echelon vehicle routing problem. *Computers & Operations Research, 103*, 198–210.

Contardo, C., Hemmelmayr, V., & Crainic, T. G. (2012). Lower and upper bounds for the two-echelon capacitated location-routing problem. *Computers & operations research, 39*, 3185–3199.

Correia, I., Gouveia, L., & Saldanha-da-Gama, F. (2008). Solving the variable size bin packing problem with discretized formulations. *Computers & Operations Research, 35* (6), 2103–2113.

Crainic, T. G., Ricciardi, N., & Storchi, G. (2009). Models for evaluating and planning city logistics systems. *Transportation science, 43*(4), 432–454.

Díaz-Ramírez, J., Zazueta-Nassif, S., Galarza-Tamez, R., Prato-Sánchez, D., & Huertas, J. I. (2023). Characterization of urban distribution networks with light electric freight vehicles. *Transport and Environment, 119*, Article 103719.

Darvish, M., Archetti, C., Coelho, L. C., & Speranza, M. G. (2019). Flexible two-echelon location routing problem. *European Journal of Operational Research, 277*(3), 1124–1136.

Desaulniers, G., Desrosiers, J., & Solomon, M. M. (2006). *Column generation*. Springer Science & Business Media. Vol. 5):.

Divieso, E., LIMA, O. F., & De Oliveira, H. C (2021). The use of waterways for urban logistics. *Theoretical and Empirical Researches in Urban Management, 16*(1), 62–85.

Enthoven, D. L., Jargalsaikhan, B., Roodbergen, K. J., Uit het Broek, M. A., & Schrotenboer, A. H. (2020). The two-echelon vehicle routing problem with covering options: City logistics with cargo bikes and parcel lockers. *Computers & Operations Research, 118*, Article 104919.

Grangier, P., Gendreau, M., Lehuédé, F., & Rousseau, L. M. (2016). An adaptive large neighborhood search for the two-echelon multiple-trip vehicle routing problem with satellite synchronization. *European Journal of Operational Research, 254*(1), 80–91.

Gu, Y., & Wallace, S. W. (2021). Operational benefits of autonomous vessels in logistics—A case of autonomous water-taxis in Bergen. *Logistics and Transportation Review, 154*, Article 102456.

Hemmelmayr, V. C., Cordeau, J. F., & Crainic, T. G. (2012). An adaptive large neighborhood search heuristic for two-echelon vehicle routing problems arising in city logistics. *Computers & operations research, 39*(12), 3215–3228.

Huang, H., Yang, S., Li, X., & Hao, Z. (2021). An Embedded Hamiltonian Graph-Guided Heuristic Algorithm for Two-Echelon Vehicle Routing Problem. *IEEE Transactions on Cybernetics*.

Janjevic, M., & Ndiaye, A. B. (2014). Inland waterways transport for city logistics: A review of experiences and the role of local public authorities. In *Urban Transport XX, 138* pp. 279–290).

Jia, S., Deng, L., Zhao, Q., & Chen, Y. (2022). An adaptive large neighborhood search heuristic for multi-commodity two-echelon vehicle routing problem with satellite synchronization. *Journal of Industrial and Management Optimization*.

Jie, W., Yang, J., Zhang, M., & Huang, Y. (2019). The two-echelon capacitated electric vehicle routing problem with battery swapping stations: Formulation and efficient methodology. *European Journal of Operational Research, 272*(3), 879–904.

Kodinariya, T. M., & Makwana, P. R. (2013). Review on determining number of Cluster in K-Means Clustering. *International Journal, 1*, 90–95.

Korff, M., Hemel, M. J., & Peters, D. J. (2022). Collapse of the Grimburgwal, a historic quay in Amsterdam, the Netherlands. *Proceedings of the Institution of Civil Engineers-Forensic Engineering, 40*(3), 1–10.

Kortmann, L., van de Kamp, M., Taniguchi, E., & Thompson, R. (2018). Towards sustainable urban distribution using city canals: The case of Amsterdam. *New opportunities and challenges* (pp. 65–83).

Leirião, L.F.L., Debone, D., Pauliquevis, T., do Rosário, N.M.É., & Miraglia, S.G.E.K. (2020). Environmental and public health effects of vehicle emissions in a large metropolis: Case study of a truck driver strike in Sao Paulo, Brazil. *Atmospheric Pollution Research*, 11, 24–31.

Li, H., Wang, H., Chen, J., & Bai, M. (2020). Two-echelon vehicle routing problem with time windows and mobile satellites. *Transportation Research Part B: Methodological, 138*, 179–201.

Li, H., Wang, H., Chen, J., & Bai, M. (2021). Two-echelon vehicle routing problem with satellite bi-synchronization. *European Journal of Operational Research, 288*(3), 775–793.

Liu, D., Yang, H., Mao, X., Antonoglou, V., & Kaisar, E. I. (2023). New mobility-assist E-grocery delivery network: a load-dependent two-echelon vehicle routing problem with mixed vehicles. *Transportation Research Record, 2677*(1), 294–310.

Maes, J., Sys, C., & Vanelslander, T. (2015). City logistics by water: Good practices and scope for expansion. *Transport of water versus transport over water* (pp. 413–437). Springer.

Mhamedi, T., Andersson, H., Cherkesly, M., & Desaulniers, G. (2022). A branch-price-and-cut algorithm for the two-echelon vehicle routing problem with time windows. *Transportation science, 56*(1), 245–264.

Miloslavskaya, S., Lukoševičienė, E., & Myskina, A. (2019). Inland waterways transport in large cities transport system: Practice and prospect.

Mirhedayatian, S. M., Crainic, T. G., Guajardo, M., & Wallace, S. W. (2021). A two-echelon location-routing problem with synchronisation. *Journal of the Operational Research Society, 72*(1), 145–160.

Municipality of Amsterdam (MoA). (2020). Analysis report Transport by Water: The blue blood circulation of Amsterdam, Available at: Https://assets.amsterdam.nl/publish/pages/862914/analyserapport_transport_over_water.pdf.

Nagata, Y., Bräysy, O., & Dullaert, W. (2010). A penalty-based edge assembly memetic algorithm for the vehicle routing problem with time windows. *Computers & operations research, 37*(4), 724–737.

Nepveu, R., & Nepveu, M. (2020). *Implementing urban waterway transport as a sustainable freight transport solution: A case study for the city of amsterdam*. TU Delft.

Paraskevopoulos, D. C., Repoussis, P. P., Tarantilis, C. D., Ioannou, G., & Prastacos, G. P. (2008). A reactive variable neighborhood tabu search for the heterogeneous fleet vehicle routing problem with time windows. *Journal of Heuristics, 14*(5), 425–455.

Perboli, G., Tadei, R., & Vigo, D. (2011). The two-echelon capacitated vehicle routing problem: Models and math-based heuristics. *Transportation science, 45*(3), 364–380.

Pina-Pardo, J. C., Moreno, M., Barros, M., Faria, A., Winkenbach, M., & Janjevic, M. (2022). Design of a two-echelon last-mile delivery model. *EURO Journal on Transportation and Logistics, 11*, 100079.

Potvin, J. Y., & Rousseau, J. M. (1995). An exchange heuristic for routeing problems with time windows. *Journal of the Operational Research Society, 46*(12), 1433–1446.

Ribeiro, G. M., & Laporte, G. (2012). An adaptive large neighborhood search heuristic for the cumulative capacitated vehicle routing problem. *Computers & operations research, 39*, 728–735.

Ropke, S., & Pisinger, D. (2006). An adaptive large neighborhood search heuristic for the pickup and delivery problem with time windows. *Transportation science, 40*, 455–472.

Savelsbergh, M. W. (1992). The vehicle routing problem with time windows: Minimizing route duration. *ORSA journal on Computing, 4*(2), 146–154.

Schneider, M., Sand, B., & Stenger, A. (2013). A note on the time travel approach for handling time windows in vehicle routing problems. *Computers & operations research, 40*(10), 2564–2568.

Shi, Y., Lin, Y., Wang, S., Wen, H., Lim, M. K., & Li, Y. (2023). A simultaneous facility location and vehicle routing problem with recyclable express packaging consideration for sustainable city logistics. *Sustainable Cities and Society, 98*, Article 104857.

Sluijk, N., Florio, A. M., Kinable, J., Dellaert, N., & Van Woensel, T. (2023). Two-echelon vehicle routing problems: A literature review. *European Journal of Operational Research, 304*(3), 865–886.

Van Der Does, J. (2019). *Assessing the impact of quay-wall renovations on the nautical traffic in amsterdam*. TU Delft.

Van Der Storm, C. P. G (2021). *Modelling the consequences of using a waterborne construction logistics system for quay wall renovations in amsterdam*. TU Delft.

Vincent, F. Y., Jodiawan, P., Hou, M. L., & Gunawan, A. (2021). Design of a two-echelon freight distribution system in last-mile logistics considering covering locations and occasional drivers. *Logistics and Transportation Review, 154*, Article 102461.

Wang, Y., Assogba, K., Liu, Y., Ma, X., Xu, M., & Wang, Y. (2018). Two-echelon location-routing optimization with time windows based on customer clustering. *Expert Systems with Applications, 104*, 244–260.

Wojewódzka-Król, K., & Rolbiecki, R. (2019). The role of inland waterway transport in city logistics. *Transport Economics and Logistics* (p. 84).

Wu, Z., & Zhang, J. (2021). A branch-and-price algorithm for two-echelon electric vehicle routing problem. *Complex & Intelligent Systems*, 1–16.

Yu, S., Puchinger, J., & Sun, S. (2020). Two-echelon urban deliveries using autonomous vehicles. *Logistics and Transportation Review, 141*, Article 102018.

Zhang, L., Ding, P., & Thompson, R. G. (2023). A stochastic formulation of the two-echelon vehicle routing and loading bay reservation problem. *Logistics and Transportation Review, 177*, Article 103252.

Zhao, Q., Wang, W., & De Souza, R (2018). A heterogeneous fleet two-echelon capacitated location-routing model for joint delivery arising in city logistics. *International Journal of Production Research, 56*(15), 5062–5080.

Zhou, L., Baldacci, R., Vigo, D., & Wang, X. (2018). A multi-depot two-echelon vehicle routing problem with delivery options arising in the last mile distribution. *European Journal of Operational Research, 265*(2), 765–778.